Mississippi State University
Scholars Junction

Theses and Dissertations | Theses and Dissertations

1-1-2017

Interrupted High-Rate Compression of Porcine Brain Tissue Utilizing the Split Hopkinson Pressure Bar Method

Haden Andrew Johnson

Follow this and additional works at: https://scholarsjunction.msstate.edu/td

Recommended Citation
Johnson, Haden Andrew, "Interrupted High-Rate Compression of Porcine Brain Tissue Utilizing the Split Hopkinson Pressure Bar Method" (2017). *Theses and Dissertations*. 2786.
https://scholarsjunction.msstate.edu/td/2786

This Graduate Thesis - Open Access is brought to you for free and open access by the Theses and Dissertations at Scholars Junction. It has been accepted for inclusion in Theses and Dissertations by an authorized administrator of Scholars Junction. For more information, please contact scholcomm@msstate.libanswers.com.

www.manaraa.com

Interrupted high-rate compression of porcine brain tissue utilizing the split Hopkinson pressure bar method

By

Haden Andrew Johnson

A Thesis
Submitted to the Faculty of
Mississippi State University
in Partial Fulfillment of the Requirements
for the Degree of Master of Science
in Biomedical Engineering
in the Department of Agricultural and Biological Engineering

Mississippi State, Mississippi

August 2017

www.manaraa.com

Copyright by

Haden Andrew Johnson

2017

www.manaraa.com

Interrupted high-rate compression of porcine brain tissue utilizing the split Hopkinson pressure bar method

By

Haden Andrew Johnson

Approved:

Lakiesha N. Williams
(Major Professor)

Rajkumar Prabhu
(Committee Member)

Jun Liao
(Committee Member)

Alicia Kathleen Olivier
(Committee Member)

Michael D. Jones
(Committee Member)

Steven H. Elder
(Graduate Coordinator)

Jason M. Keith
Dean
Bagley College of Engineering

www.manaraa.com

Name: Haden Andrew Johnson

Date of Degree: August 11, 2017

Institution: Mississippi State University

Major Field: Biomedical Engineering

Major Professor: Dr. Lakiesha N. Williams

Title of Study: Interrupted high-rate compression of porcine brain tissue utilizing the split Hopkinson pressure bar method

Pages in Study 57

Candidate for Degree of Master of Science

Traumatic brain injury (TBI) is a growing concern among American citizens and globally. This study proposes the use of a novel mechanical testing method for interrupting adult porcine brain tissue while under varying levels of high rate compressive strain to better understand the mechanical response of brain while under TBI inducing conditions. Testing was performed using a polymeric Split Hopkinson Pressure Bar (SHPB) along with customized attachments developed in-house to interrupt tissue samples at strain levels of 15%, 30%, and 40% while being compressed at strain rates of 650, 800, and 900 s^{-1}. Following interruption, the samples were chemically fixed in preparation for histological processing. Microscopy techniques were used to examine the microstructure of the deformed tissue samples and measure the area fraction of their neural constituents. The combination of both the mechanical and microstructural responses of the brain tissue allowed for the development of a structure-property relationship.

www.manaraa.com

DEDICATION

I dedicate this work to all my friends and classmates I have gained over my six years at Mississippi State during my undergraduate and graduate careers. They know how much time and effort I have put into this pursuit because they have been right there alongside. I also want to acknowledge all my teachers and professors, both past and present, that have given me the knowledge and instruction to get me to where I am today. I would not have gotten this far in life without the love and support of my family. They literally made me into the man that I am now. I am proud and grateful for my dad who served our country as an active duty service member in the US Army. His service led to me being able to receive his GI Bill, so I would not have to worry as much about the financial burdens of acquiring my undergraduate degree. I especially want to dedicate this work to my mom. She is my number one fan and supporter. She has always been there to push me to do my absolute best in anything I attempt and to always do what is right. I find myself to be more and more like her each day, and for that, I will always be grateful. Finally, I would like to thank Mary. She is my best friend and has been there through the ups and downs supporting me in this entire process. Without her love and caring, I doubt this document would have ever been finished. I just hope that I was able to help her as much with surviving nursing school as she was in helping me survive graduate school.

www.manaraa.com

ACKNOWLEDGEMENTS

Material presented in this paper is a product of the CREATE-GV Element of the Computational Research and Engineering Acquisition Tools and Environments (CREATE) Program sponsored by the U.S. Department of Defense HPC Modernization Program Office. This effort was sponsored under contract number W912HZ-13-C-0037.

I would like to thank the Center for Advanced Vehicular Systems (CAVS) and the Agricultural and Biological Engineering Department at Mississippi State University (MSU) for use of their laboratories and facilities in support of this work. I would also like to thank Sansing Meat Processing for their assistance with acquiring adequate test specimens. Additionally, I would like to thank MSU's College of Veterinary Medicine Diagnostic Laboratory Services (CVM-DLS) for histological processing and staining of tissue samples.

I would like to thank Dr. Wilburn Whittington and Mr. Jonathon Miller for their assistance with all the Hopkinson bar testing that was conducted during this research. Also, I would like to acknowledge Dr. Jim Cooley at MSU's College of Veterinary Medicine for his assistance in explaining the porcine brain extraction procedure, Mr. Stephen Horstemeyer at CAVS for his training on the machining equipment necessary to manufacture the interruption attachments, Dr. David Francis for assistance in using his Split Hopkinson Pressure Bar Graphical Analysis Tool software for data processing, and Dr. Steve Elder for instructional training on the light microscope that was used for all

www.manaraa.com

microstructural analysis. Finally, I would like to thank the members of my graduate committee for their time and efforts in advising the work that was necessary for the completion of this thesis.

www.manaraa.com

TABLE OF CONTENTS

www.manaraa.com

www.manaraa.com

LIST OF TABLES

www.manaraa.com

LIST OF FIGURES

www.manaraa.com

www.manaraa.com

CHAPTER I

INTRODUCTION

1.1 Background

The central nervous system (CNS) is composed of the brain and spinal cord that work together with the purpose of maintaining control over all the complex mechanisms in the body that are essential to survival. The brain acts as a central processor interpreting and making decisions about the different signals and inputs it receives, and the spinal cord acts as a relay mechanism delivering and sending those signals to and from the brain. The tissues in the CNS are composed of nerve cells, or neurons, and numerous types of support cells called glial cells (Blumenfeld, 2010). Neurons are able to communicate with one another via signals that are transported along extensions called axons (Blumenfeld, 2010). These axons can be unmyelinated or myelinated to modify how signals are sent along them. Myelinated axons, like the one in Figure 1.1, are surrounded in a thick layer of fatty white insulation formed by a specific type of glial cells called Schwann cells (Thibodeau and Patton, 2008). In the brain, regions concentrated with myelinated axons are termed white matter, and regions that lack much myelination are classified as gray matter as shown in Figure 1.2 (Thibodeau and Patton, 2008).

www.manaraa.com

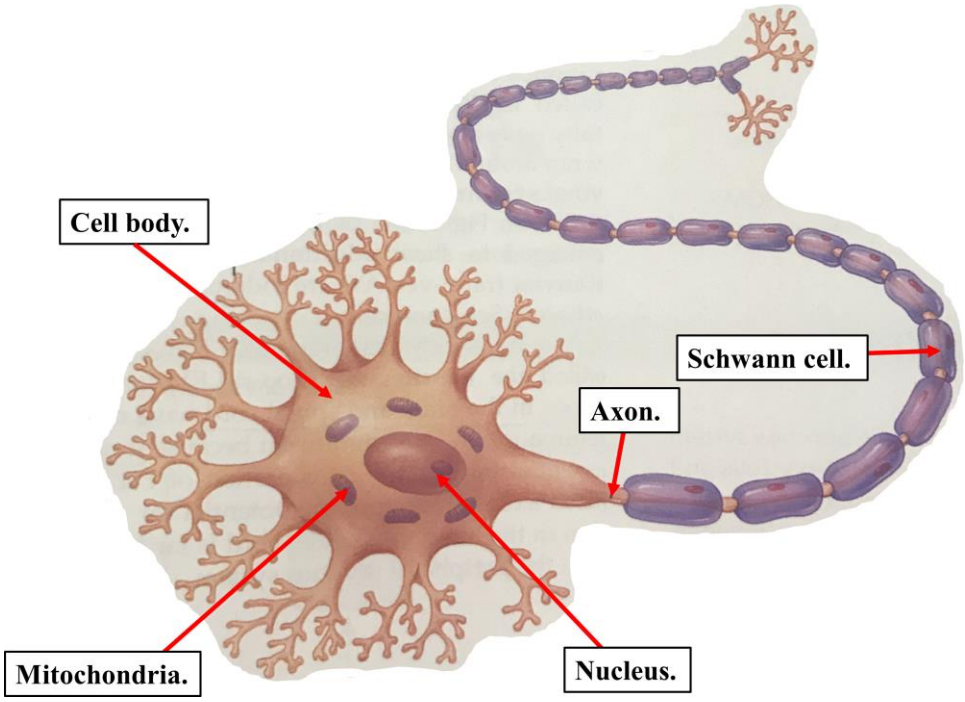

Figure 1.1 Typical neuron cell.

The axon extends from the cell body to allow for communication with neighboring neurons. The axon pictured here is myelinated due to the presence of Schwann cells. Adapted from (Thibodeau and Patton, 2008).

www.manaraa.com

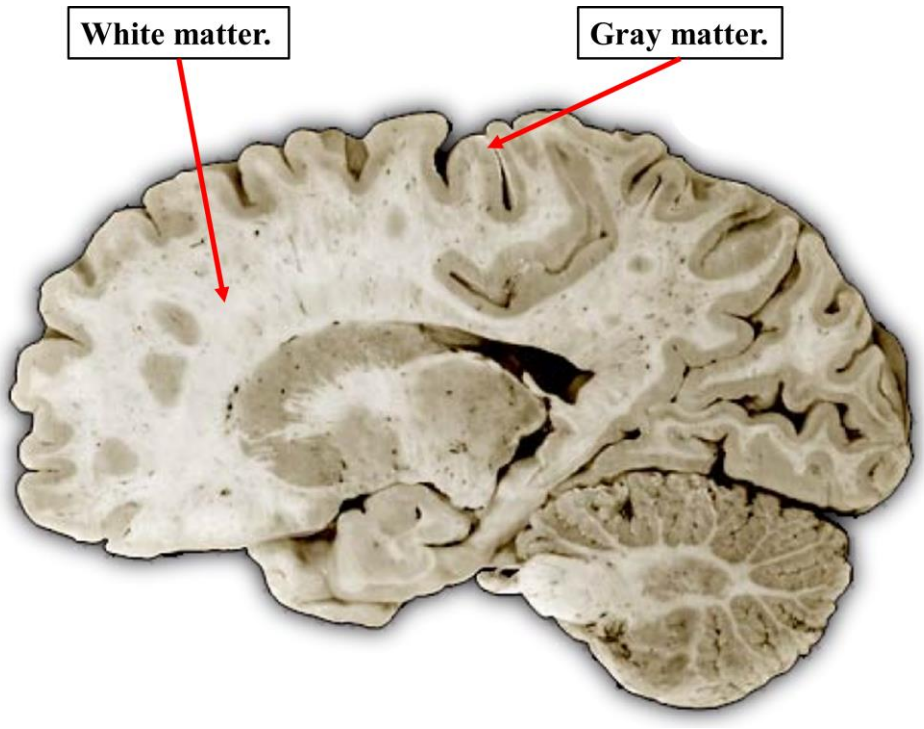

Figure 1.2 Sagittal view of brain tissue.

The different regions of white and gray matter can be clearly seen. Adapted from (Williams and White, 2013).

Unfortunately, the operation of this highly complex, yet organized system can become impaired whenever the brain is injured, especially as a result of high impact injuries associated with traumatic brain injury (TBI). A TBI is often defined as a physiological disruption of brain function that is caused by the head striking or being struck by an object or if the brain undergoes severe acceleration or deceleration (Kay et al., 1993). When a person receives a TBI, it often leads to physical impairments, cognitive deficits, and behavioral changes (Kay et al., 1993). These symptoms can sometimes be treated, but in many instances, will lead to permanent changes in the life of the patient.

www.manaraa.com

1.2 TBI Statistics

There are an estimated 1.7 million occurrences of TBI in the United States (US) each year. The most prevalent cause of these injuries is the result of falls followed by motor vehicle accidents, patients being struck by an object, and physical assaults. TBI annually results in 52,000 deaths, accounting for one third of all injury related deaths in the US. (Faul et al., 2010)

TBI is also a prevalent cause of injury among US military members, both deployed and stationed at home. Between the years of 2000 and 2013, when Operation New Dawn (OND, Iraq), Operation Iraqi Freedom (OIF, Iraq), and Operation Enduring Freedom (OEF, Afghanistan) were ongoing, over 280,000 service members sustained a TBI (Fischer, 2014). Over 7,000 of the TBIs that occurred were classified as "severe or penetrating," which means that the dura mater, a membrane that surrounds the brain tissue, was actually penetrated by some form of shrapnel (Risdall and Menon, 2011; Fischer, 2014). The major cause of TBI in a war zone is typically due to a blast or explosion often caused by an improvised explosive device (IED) (Okie, 2005; Risdall and Menon, 2011). The recent increase in worldwide terrorist attacks also brings an increase in the likelihood that civilians may also be susceptible to blast-related related TBI (Rosenfeld et al., 2013). TBI presents itself as an alarming issue, and steps must be taken in order better control this type of injury.

1.3 Previous Studies on TBI and Brain Tissue Mechanics

To help prevent TBI in the future, improvements can be made to increase the safety of both civilian and military vehicles and improve the effectiveness of personal protective equipment used by athletes, workers in hazardous environments, or military

www.manaraa.com

and police personnel. Finite element (FE) models are often used to simulate the mechanical response of brain tissue when developing new products and surgical procedures (Miller and Chinzei, 1997; Miller, 1999; Miller et al., 2000; Chen et al., 2014). By more accurately modeling the mechanical properties of the brain, the overall effectiveness of these FE models can be improved.

Numerous studies have been completed to better understand the various mechanical properties of brain tissue; however, there is often much variation in observed results due to vast differences in experimental testing methods used by different groups. Brain tissue has been tested under quasi-static and dynamic conditions at strain rates ranging from 0.00625 s^{-1} to 3000 s^{-1} (Miller and Chinzei, 2002; Pervin and Chen, 2009; Begonia et al., 2010; Prabhu et al., 2011; Thibault P. Prevost et al., 2011; Zhang et al., 2011; Clemmer et al., 2016). All mechanical results verify that brain is a viscoelastic material and shows significant strain rate dependence. The Poisson's ratio for brain tissue has been identified to be approximately 0.5 (Miller et al., 2000; Chen et al., 2014). Studies on the differences between white and gray matter show that white matter is slightly less homogeneous than gray matter, but it is also stiffer in nature (Pervin and Chen, 2009; van Dommelen et al., 2010).

In one study by Begonia et al., the microstructural changes of brain tissue under compressive loading were quantified to develop a more comprehensive understanding of the overall damage that occurs during brain tissue deformation (Begonia et al., 2010). The samples in this study were only tested at quasi-static strain rates, which are much lower than those that are typically associated with TBI. This study proposes to use methods similar to those implemented by Begonia et al. to interrupt brain tissue

www.manaraa.com

specimens for microstructural analysis, but samples will be loaded at high strain rates to better simulate loadings experienced during blasts and other high impact events. By studying the microstructural response of brain tissue under deformation at high strain rates, the relative severity of TBI can be evaluated further.

1.4 SHPB Background

Initial investigation into the mechanical response of materials at very high strain rates was performed by Hopkinson in 1914 (Hopkinson, 1914). He developed a method that could measure the amount of pressure produced by explosions or the impact of ballistic projectiles. It involved impacting a steel rod with a projectile and measuring the amount of pressure that was produced in the rod over time. Later, Kolsky modified Hopkinson's testing method and used multiple bars to create the first Split Hopkinson Pressure Bar (SHPB) or Kolsky bar, and it was used to measure the mechanical response of various rubbers, plastics, and metals (Kolsky, 1949). Eventually, Zhao et al. further modified the SHPB by building the bars out of viscoelastic material (Zhao et al., 1997). This change was made because viscoelastic bars have a lower impedance than that of the steel bars that had previously been used. Low impedance bars allowed for better test results of lower impedance materials such as various foams. These viscoelastic bars would also prove to be very valuable in the testing of extremely soft biological tissues (Sharma et al., 2002; Van Sligtenhorst et al., 2006; Prabhu et al., 2011).

1.5 Specific Aims

To truly understand the mechanical properties of biological tissues, such as the brain, connections must be made between the brain's response to damage at both the

www.manaraa.com

tissue and cellular levels (Jeronimidis, 2000). In this study, we have designed and developed a novel method for performing interrupted compression tests on soft biological tissues utilizing the SHPB method. Interruption of the mechanical tests in this study allowed for the tissue to be fixed at the pre-set strain levels and histological analysis to be done to capture the brain tissue microstructure at various strain levels and strain rates. This provided another metric to quantify the amount of damage occurring at varying strain rates and strain levels and correlate with the mechanical response. Area fraction of neural constituents was used as a quantifiable measure to determine the change in the tissue at the different testing parameters. These methods and techniques were used to meet the following specific aims of this study:

1. Perform high rate mechanical testing on porcine brain tissue utilizing the SHPB to verify the material exhibits strain rate dependent viscoelastic behavior.
2. Develop a novel testing method that can be adapted to the SHPB and allows for interrupted compression testing at desired levels of strain.
3. Utilize histological techniques to analyze the microstructural damage that occurs in brain tissue that has been interrupted while under high rate compressive loading.
4. Use the mechanical and microstructural information gathered to better explain the damage evolution the brain undergoes from conditions that would result in a TBI.

www.manaraa.com

CHAPTER II

METHODS

2.1 Sample Preparation

Adult pig heads were obtained from a local abattoir (Sansing Meat Service, Maben, MS, USA). The heads were stored in an iced container and transported to the BSL-2 laboratory at the Agricultural and Biological Engineering building at Mississippi State University (MSU). Intact porcine brains were extracted from the heads and separated into the left and right hemispheres through halving the corpus callosum. All meningeal layers were carefully removed to isolate the desired neural tissue. Cylindrical samples of mixed gray and white matter were resected from the superior cortical region of the frontal and parietal lobes using a custom stainless steel punch. Samples were taken from both the right and left brain hemispheres. The cylindrical samples had a diameter of 20 mm and, using a surgical scalpel, were cut to 10 mm in length to provide a 2:1 aspect ratio. An example of a typical sample can be seen in Figure 2.1. The samples were then wrapped in gauze soaked in 0.01 M Phosphate Buffered Saline (PBS) to prevent any dehydration, and they transported to the Center for Advanced Vehicular Systems (CAVS) at MSU for mechanical testing. All tests were completed within three hours post mortem to limit any effects of tissue deterioration and maintain consistent results across all samples.

www.manaraa.com

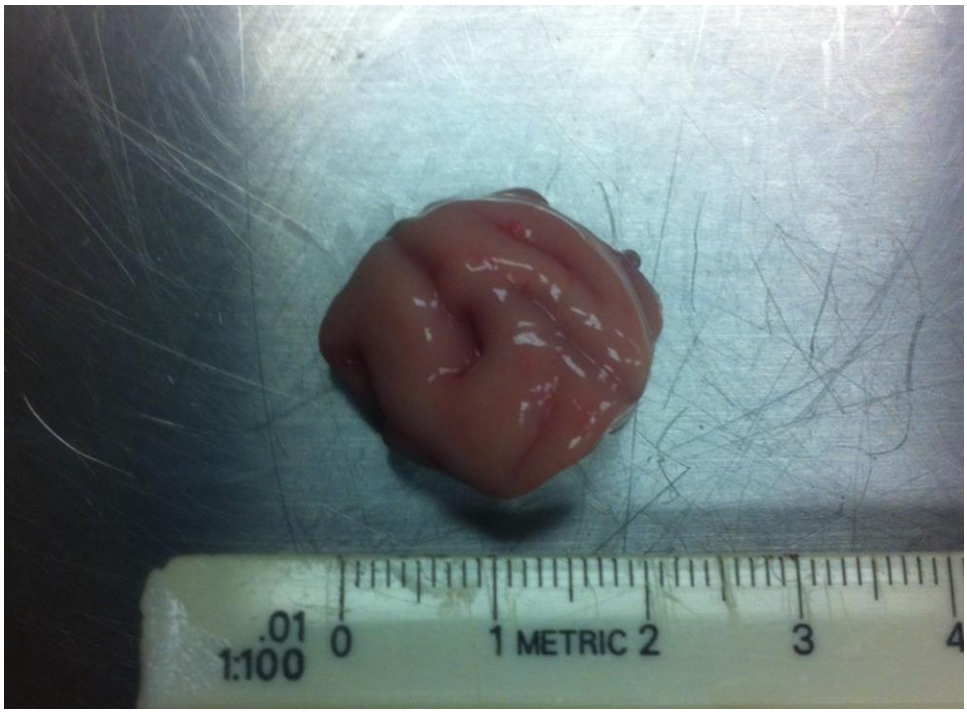

Figure 2.1 Brain tissue sample.

The cylindrical sample is composed of both gray and white matter and characterized by the sulci and gyri. The diameter is ~20 mm.

2.2 SHPB Testing

A SHPB was chosen for compression testing due to its capability in achieving high strain rates that could simulate conditions like those that occur during severe automotive accidents and other high impact events (Hopkinson, 1914; Kolsky, 1949). A custom-built polymeric SHPB housed at CAVS was used to test the brain tissue samples. The testing techniques used with this particular SHPB were adapted from similar studies that have previously used it (Prabhu et al., 2011; Clemmer et al., 2016). A polymeric SHPB was used in order to provide better test results considering that the polymer impedance is closer to that of soft biological tissues as opposed to metallic bars with a high impedance (Zhao et al., 1997). The main components of the SHPB used were a

www.manaraa.com

striker bar, incident bar, and transmitted bar as indicated in Figure 2.2. The samples were placed between the incident and transmitted bars, and the striker bar was loaded into a chamber that was connected to a pressurized gas cylinder and used as the firing mechanism. Strain gages were adhered to the incident and transmitted bars to capture the incident, reflected, and transmitted waves that were produced during the tests. The waves were then analyzed with the Split Hopkinson Pressure Bar Graphical Analysis Tool to produce stress-strain data for the mechanical tests (Francis et al., 2017). Full compression tests, to failure, were initially performed to evaluate the mechanical response of the brain tissue. Tests were conducted at strain rates of 650, 800, and 900 s^{-1}. Additional information on the SHPB and wave analysis used in this study can be found in Appendix A.

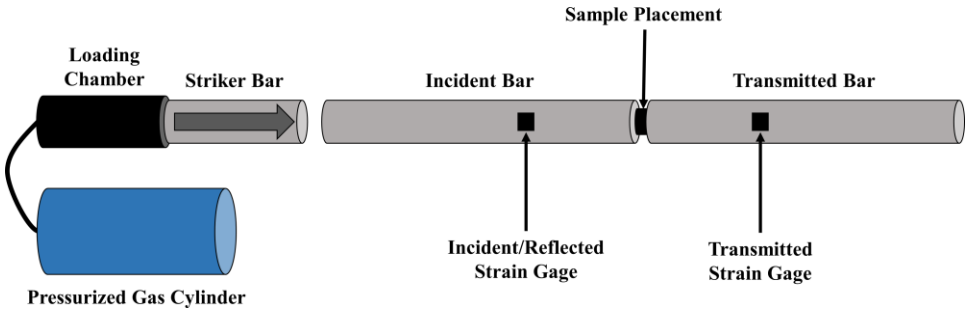

Figure 2.2 SHPB schematic.

The different parts that are illustrated are the three bars that compose the device, the components of the pneumatic pressure system, locations of the strain gages, and sample placement. The arrow on the striker bar indicates the direction of loading.

2.3 Interruption Testing

To perform the interruption tests necessary for histological analysis of the brain tissue, custom attachments were designed and fabricated. Cylindrical disks, 60 mm in

www.manaraa.com

diameter and 13 mm in thickness, were cut from a sheet of polycarbonate, similar to the material of the polymeric SHPB. Wells were then machined on either side of the disks as depicted in Figure 2.3. The wells on one side of the disks were made to be 38.1 mm in diameter and 3 mm deep in order for them to fit firmly onto the ends of the incident and transmitted bars. The wells on the opposite sides were made 40 mm in diameter to allow for unconfined compression of the brain samples, and they were cut to various depths that corresponded to strain levels of 15, 30, and 40%. These desired levels of strain meant that the brain tissue samples would be allowed to deform from an original height of 10 mm to heights of 8.5, 7, and 6 mm. Sections of the rings surrounding the specimen wells were removed to create slots like the ones in Figure 2.4. The slots would allow formalin to enter and penetrate the tissue after completing each interrupted test. One pair of disks like the ones pictured in Figure 2.5 was necessary for successful completion of each interruption test.

www.manaraa.com

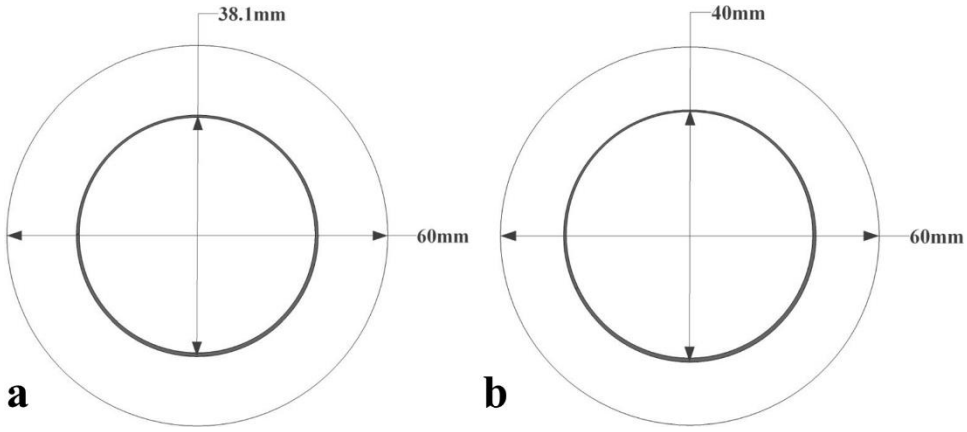

Figure 2.3 Interruption attachments schematic.

(a) The wells on one side of the interruption attachments were cut to have a diameter of 38.1 mm and a depth of 3 mm. These dimensions allowed for the attachments to fit securely onto the SHPB. (b) On the opposite side of each attachment, the wells were cut to 40 mm in diameter in order to allow for unconfined compression of the 20 mm diameter brain tissue samples. The depths of the wells on this side varied to allow for compression interruption at strain levels of 15%, 30%, and 40%.

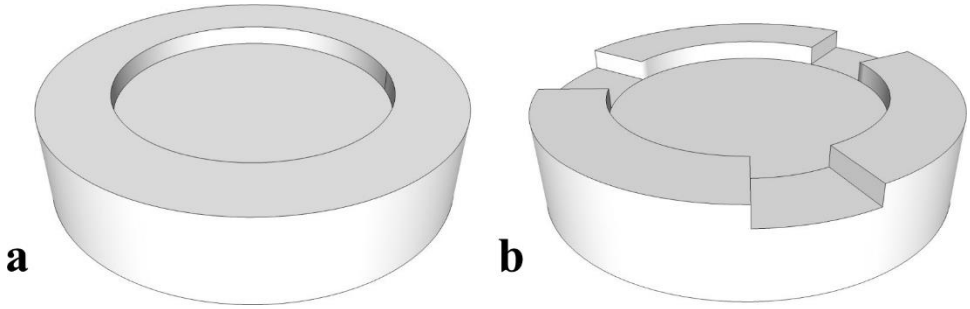

Figure 2.4 Interruption attachments with and without slots.

In each pair of attachments used during interruption testing, (a) one would have a full ring around the well, and (b) the other would have sections of material removed to create slots. The three slots were used on the outer ring to allow for formalin to enter the attachments and penetrate the brain tissue sample during chemical fixation.

www.manaraa.com

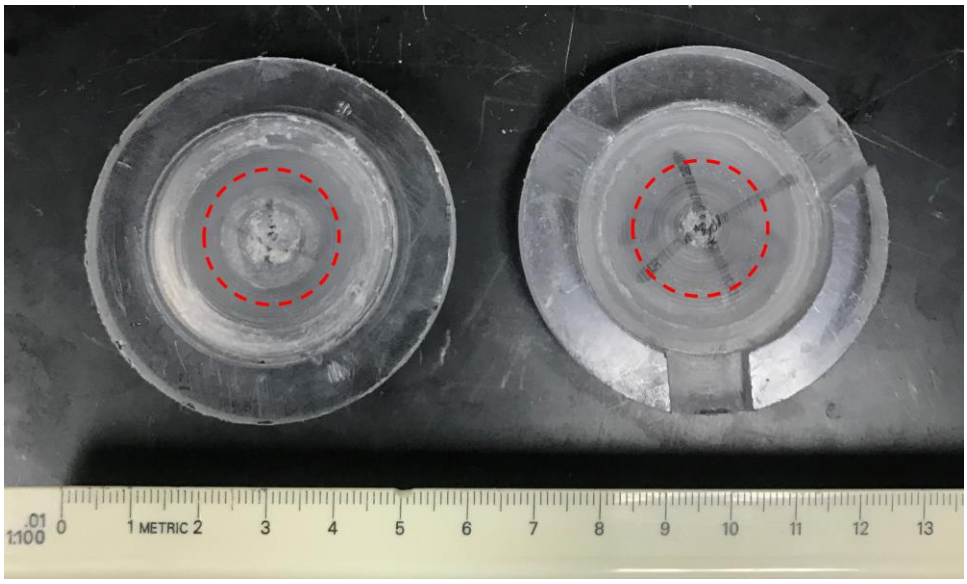

Figure 2.5 Interruption attachment set.

Pairs of custom built interruption attachments were necessary for interruption testing with the SHPB. The dashed red circles represent placement of the 20 mm diameter porcine brain samples inside the attachments.

To perform the interruption tests, double-sided adhesive tape was placed on the rings of the attachments surrounding the specimen wells. One attachment was fitted to the incident bar, the other to the transmitted bar and the sample placed in the wells between them. The SHPB was then pressurized to predetermined (psi) levels to achieve the desired strain rates of 650, 800, and 900 s^{-1} (30 psi was correlated to be 650 s^{-1}, 45 psi was correlated to be 800 s^{-1}, and 60 psi was correlated to be 900 s^{-1}). Upon releasing the gas, the samples were compressed until the pair of attachments made contact with each other and interrupted the test. The double-sided adhesive tape ensured that the attachments would remain in contact with one another and hold the samples in the partially compressed state as shown in Figure 2.6. After each test, the attachments, with

www.manaraa.com

the sample still compressed inside, were removed from the SHPB and placed into a bath of 10% neutral buffered formalin solution to allow for tissue fixation in the compressed state. Formalin was able to reach the tissue held inside the attachments because of the slots added to them when constructed.

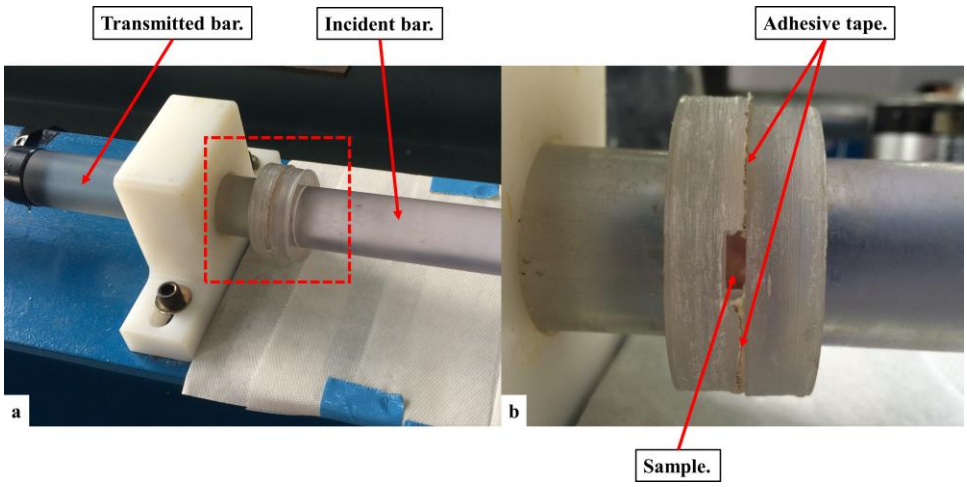

Figure 2.6 Interruption attachments on SHPB.

(a) A pair of interruption attachments affixed to the ends of the incident and transmitted bars. (b) Interruption attachments configuration following a compression test. The adhesive tape is holding the two attachments together keeping the brain tissue sample in a compressed state and preventing relaxation. The sample can be seen still intact through one of the slots.

2.4 Sample Sectioning

Samples remained in their compressed state inside the interruption attachments for 7 days before removal to provide sufficient time for fixative penetration into the interrupted samples. After this period, samples were removed and sectioned in preparation for microstructural analysis. Slices were removed from the central portions of the samples in the longitudinal direction in order to look at the deformation of the neural

www.manaraa.com

constituents parallel to the direction of loading. An example of the sectioning procedure used can be seen in Figure 2.7.

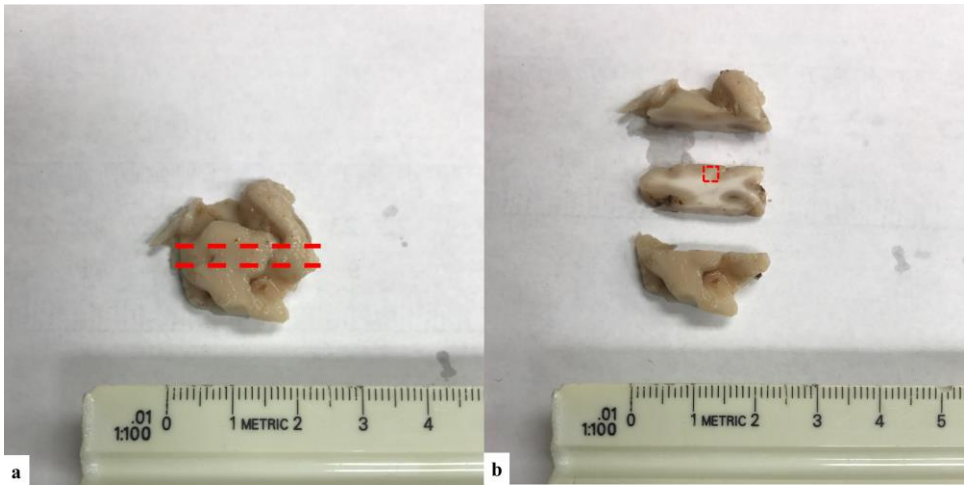

Figure 2.7 Tissue sectioning example.

(a) Overhead view of compressed sample after formalin fixation. The dashed lines indicate the location of slices that were made during sectioning procedure. (b) Central portion of tissue sample that has been excised for staining. The dashed box on the sample indicates the typical region that microstructural images were captured for use in image analysis.

2.5 Staining and Microscopy

After sectioning, the samples were placed in tissue cassettes and taken to MSU's College of Veterinary Medicine Diagnostic Laboratory Services (CVM-DLS) for staining with Haemotoxylin and Eosin (H&E) in addition to Luxol fast blue (LFB) counterstained with cresyl echt violet. H&E was chosen due to its common usage when analyzing the microstructure of biological tissues. Results from the H&E stain are shown in Figure 2.8. The combination of LFB and cresy echt violet were chosen due to their ability to differentiate the gray and white matter sections of neural tissue and identify cells. LFB is

www.manaraa.com

effective at staining the myelinated axon fibers, which are abundant in areas of white matter, blue in color. The cresyl counterstain was used to help identify neural and glial cells as shown in Figure 2.9. A Leica DM2500 light microscope and the DFC420 C Digital Camera system (Leica Microsystems, Wetzlar, Germany) were used in conjunction to capture images at 10x magnification of the uppermost central portions of the tissue sections. This region was chosen because it was located at the centermost point of the interruption attachments at the time of loading and would best represent the tissue deformation due to compression.

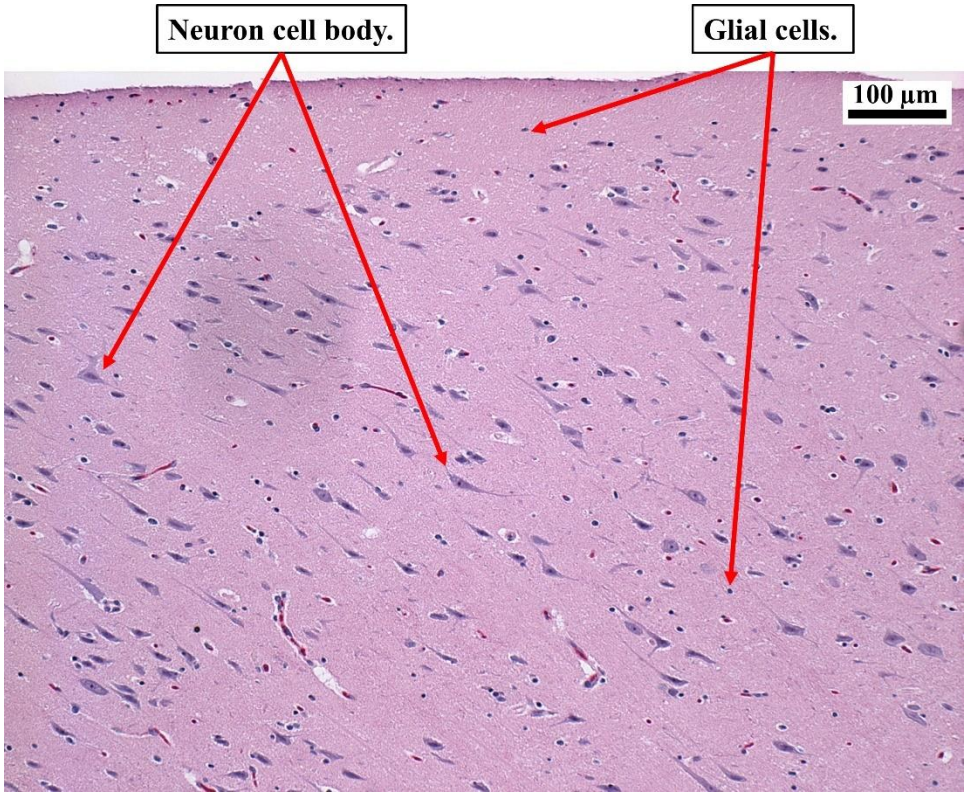

Figure 2.8 Light micrograph of H&E stained brain tissue.

Image is at 10x magnification. The background is stained pink. Cells are stained a dark purple. A scale bar is included for reference.

www.manaraa.com

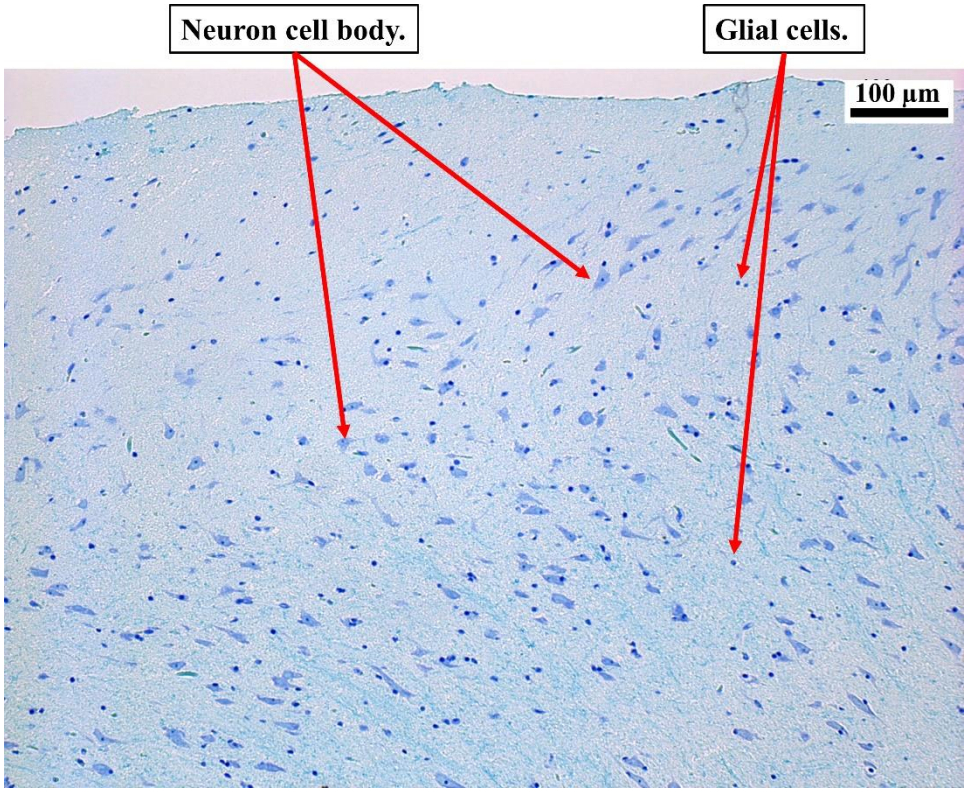

Figure 2.9 Light micrograph of LFB stained brain tissue.

Image is at 10x magnification. The background is stained light blue, and the blue hue gets darker around areas of higher myelin concentration. Cells are stained a darker blue/purple. A scale bar is included for reference.

2.6 Image Analysis

The microstructural feature of interest was the amount of compaction observed in the neural constituents of the tissue. This feature was correlated with level of compression to provide insight on physical tissue changes while under impact. Neurons and glial cells were analyzed using ImageJ software (National Institutes of Health, Bethesda, MD, USA). The area fraction of neural and glial cells from each image was measured together. Area fraction was chosen as a quantifiable parameter that could be

www.manaraa.com

used as a comparison between the tissue sections at different levels of strain and strain rates.

In an effort to increase accuracy of results from image analysis procedures, Poisson's ratio was taken into consideration prior to measuring area fraction. Poisson's ratio for brain tissue has been experimentally determined to be approximately 0.5 (Miller et al., 2000; Chen et al., 2014). This results in the diameter of the samples increasing by 50% of the amount of height reduction due to compression. Ultimately, the histology samples have a reduced cross sectional area with a reduced height and increased width. To account for this phenomenon, images were cropped according to these percentage size changes before they were analyzed. Images of the control samples measured 2591x1938 pixels and were left alone. Applying Poisson's ratio for brain tissue to images of samples that were compressed to 15, 30, and 40% strain resulted in image dimensions being changed to 2785x1685, 2980x1491, and 3109x1384, respectively to account for changes as a result of compression. Multiple images of the interrupted samples were then spliced together using the MosaicJ plugin (Ecole Polytechnique Federale De Lausanne, Lausanne, Switzerland) in ImageJ to be large enough to crop them to the proper dimensions.

After initial splicing and sizing was performed, the images were opened in ImageJ, and the split channels function was used to split the image into a red-green-blue stack. The green channel was utilized to differentiate the neural constituents from background matter. Any blood vessels or outlier artifacts that were not neural or glial cells were removed using ImageJ's cutting tools. The threshold of the green channel image was adjusted to isolate only the neural and glial cells. The threshold value used for

www.manaraa.com

each image was determined by visual comparison with the original image. Outlier removal and threshold adjustments were repeated until all neural and glial cells were isolated. The particle analysis tool was then used to calculate the area fraction of the neural constituents for the image. Masks and outlines were also produced to further ensure that only neural and glial cells were being counted in the analysis. The micrographs from the LFB stained slides were used for the image analysis procedures due to the ease of differentiating white and gray matter. Additionally, the light blue hue of the stain made isolation of the cells during threshold adjustment simpler and more precise. An example of the image analysis procedure used is shown in Figure 2.10.

www.manaraa.com

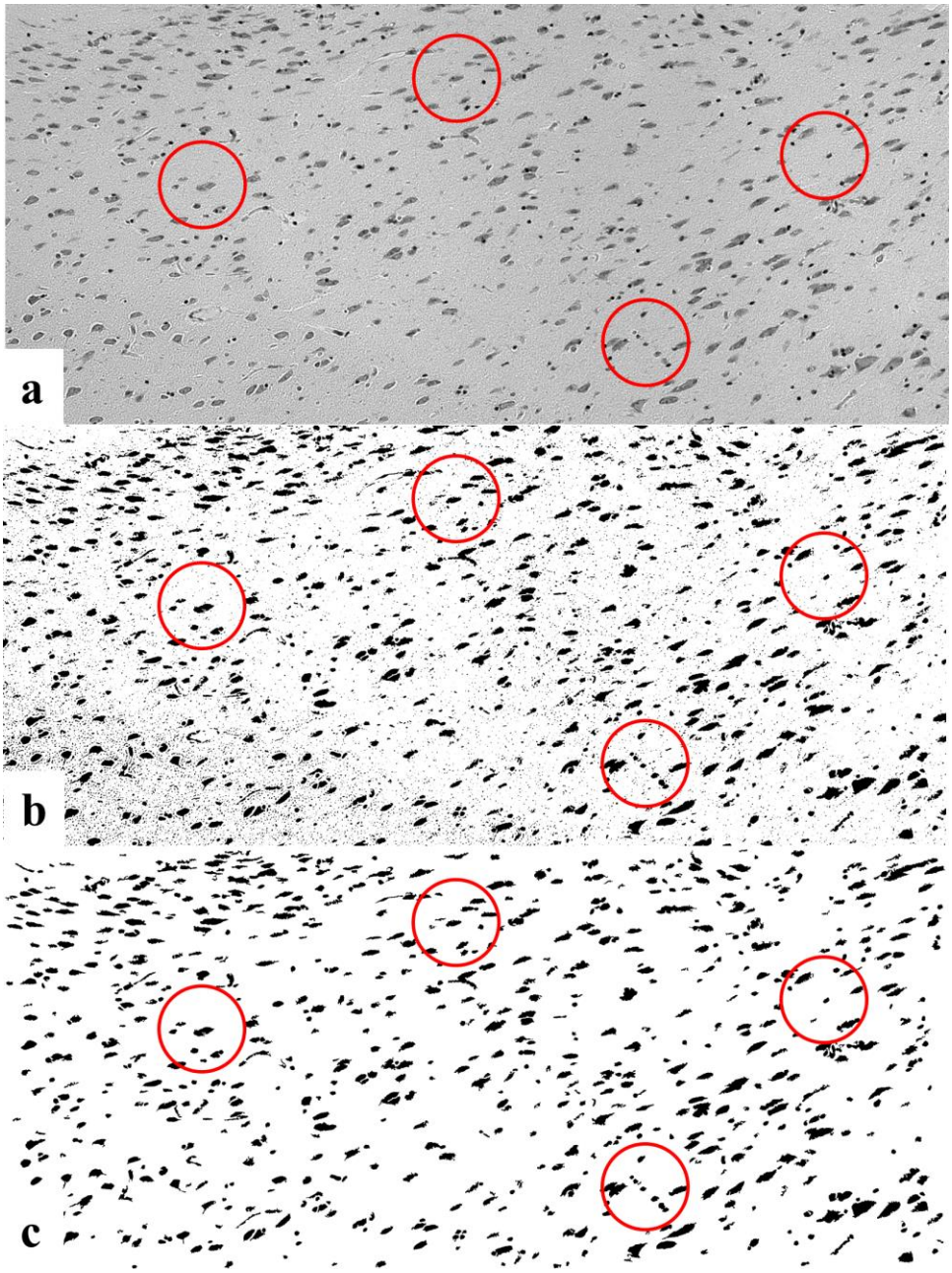

Figure 2.10 Image analysis procedure example.

(a) Green channel isolation of micrograph to convert it to an 8-bit binary file. (b) Threshold adjusted image. The threshold was adjusted to a range that removed most of the background from the image to help isolate the neural constituents. (c) Mask of image following image analysis procedure. Particles were counted within a specific size range based on pixel size to only allow neuron or glial cells to be accounted for. The circles are used to highlight regions where cells were identified in the original micrograph and verify that the image analysis procedure preserved features from the original micrographs. Particle sizes range from a few microns to approximately 100 microns.

www.manaraa.com

CHAPTER III

RESULTS

3.1 SHPB Testing

Initial compression tests were performed to failure with the SHPB to determine the mechanical response of the brain tissue at strain rates of 650 s^{-1}, 800 s^{-1}, and 900 s^{-1}. Resulting stress-strain plots from these tests are shown in Figure 3.1. Only the mechanical response after 10% strain was reported due to the samples not being at equilibrium. This criteria must be met to ensure accuracy of results when dealing with SHPB testing of viscoelastic samples (Zhao et al., 1997; Sharma et al., 2002). The results of these tests verify that the brain tissue exhibited nonlinear viscoelastic behavior and strain-rate dependence. The maximum stresses and tangent moduli were also analyzed at the strain levels of 15%, 30%, and 40% where the samples would be interrupted for microstructural analysis. The lowest stress value of 0.013 ± 0.004 MPa was given at 15% strain when compressed at a strain rate of 650 s^{-1}. The highest stress value, 0.078 ± 0.018 MPa, was for the samples compressed at 900 s^{-1} to 40% strain. When evaluating the tangent moduli that were calculated, the values get increasingly larger at each of the strain levels as the strain rate is increased. This helps to verify the brain's strain rate dependence. These results are summarized in Tables 3.1 and 3.2.

www.manaraa.com

Table 3.1 Maximum stresses from stress-strain data.

Strain Rate	Strain Level		
-	15%	30%	40%
650 s^{-1}	0.013 ± 0.004	0.025 ± 0.011	0.040 ± 0.018
800 s^{-1}	0.030 ± 0.020	0.030 ± 0.024	0.048 ± 0.032
900 s^{-1}	0.034 ± 0.056	0.051 ± 0.012	0.078 ± 0.018

The average maximum stresses in MPa were determined at the strain levels where samples were interrupted for microstructural analysis (n = 4).

Table 3.2 Tangent moduli from stress-strain data.

Strain Rate	Strain Level		
-	15%	30%	40%
650 s^{-1}	0.087 ± 0.029	0.084 ± 0.038	0.099 ± 0.044
800 s^{-1}	0.200 ± 0.133	0.100 ± 0.080	0.120 ± 0.080
900 s^{-1}	0.224 ± 0.056	0.171 ± 0.039	0.196 ± 0.044

The average tangent moduli in MPa were determined at the strain levels where samples were interrupted for microstructural analysis (n = 4).

www.manaraa.com

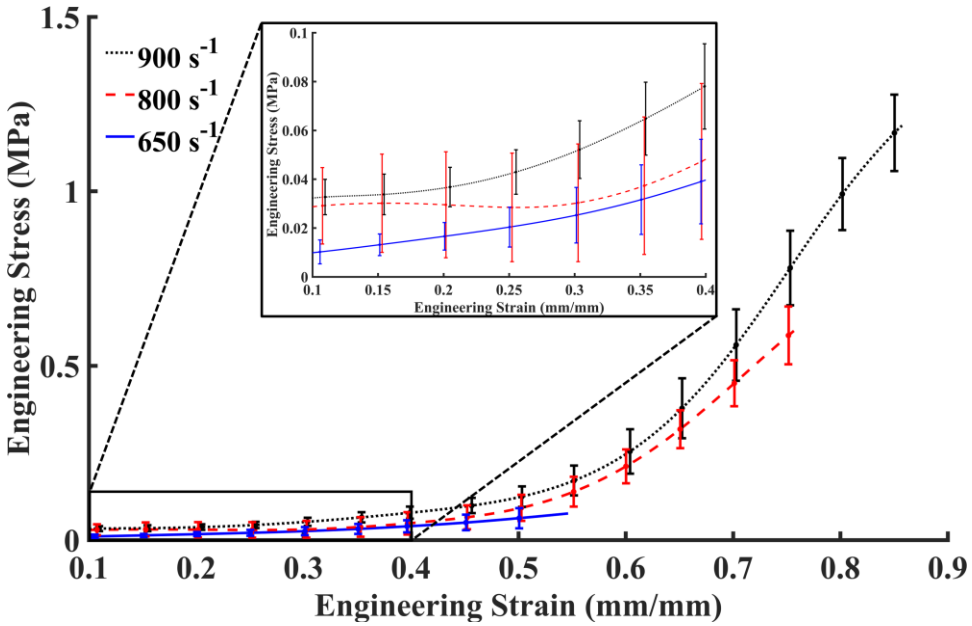

Figure 3.1 Engineering stress-strain behavior for porcine brain tissue compressed at rates of 650 s^{-1}, 800 s^{-1}, and 900 s^{-1}.

The region between 10% and 40% strain, used with microstructural analysis, is magnified. Experimental standard deviation is expressed by error bars.

3.2 Interruption Tests

The interruption tests were performed to compress the brain tissue samples to desired levels of strain and fix them to acquire interrupted tissue samples. The samples were compressed at the same strain rates as the full compression tests, but they were interrupted at strain levels of 15, 30, and 40%. Micrographs from the interrupted tests are shown stained with H&E in Figures 3.2-3.4, and those stained with LFB are in Figures 3.5-3.7. The LFB stained micrographs of the interrupted samples were combined with the mechanical data collected from the compression tests to failure to show the structure-property relationship between the mechanical response and the microstructural changes. Figure 3.8 shows a comparison of the undamaged tissue microstructure with the

www.manaraa.com

microstructure of samples compressed to 40% strain across the different strain rates. Figure 3.9 shows micrographs from samples all along the stress-strain curve that were compressed at a strain rate of 650 s^{-1}. This helps to demonstrate the damage evolution that is occurring as the tissue is compressed to higher levels of strain. Figures 3.10 and 3.11 show micrographs that correspond to the stress-strain response at strain rates of 800 s^{-1} and 900 s^{-1}, respectively.

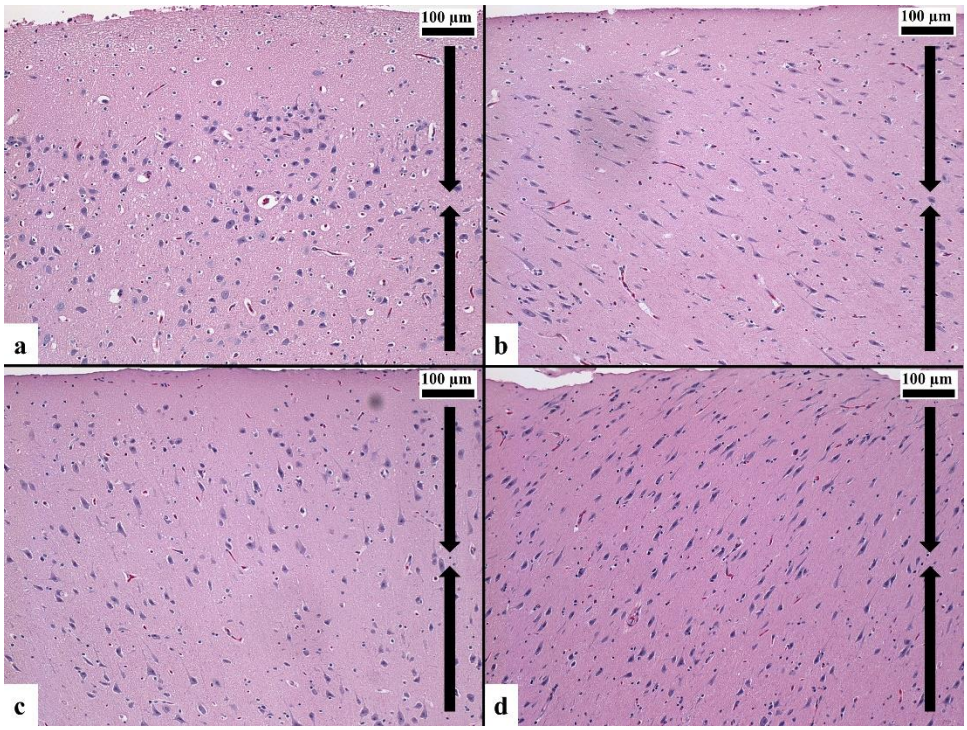

Figure 3.2 H&E stained brain tissue compressed at 650 s^{-1}: (a) An uncompressed control sample, (b) Interruption at 15% strain, (c) Interruption at 30% strain, and (d) Interruption at 40% strain.

The arrows on each image indicate the direction of compressive loading. A scale bar is included for reference. All images were taken at 10x magnification.

www.manaraa.com

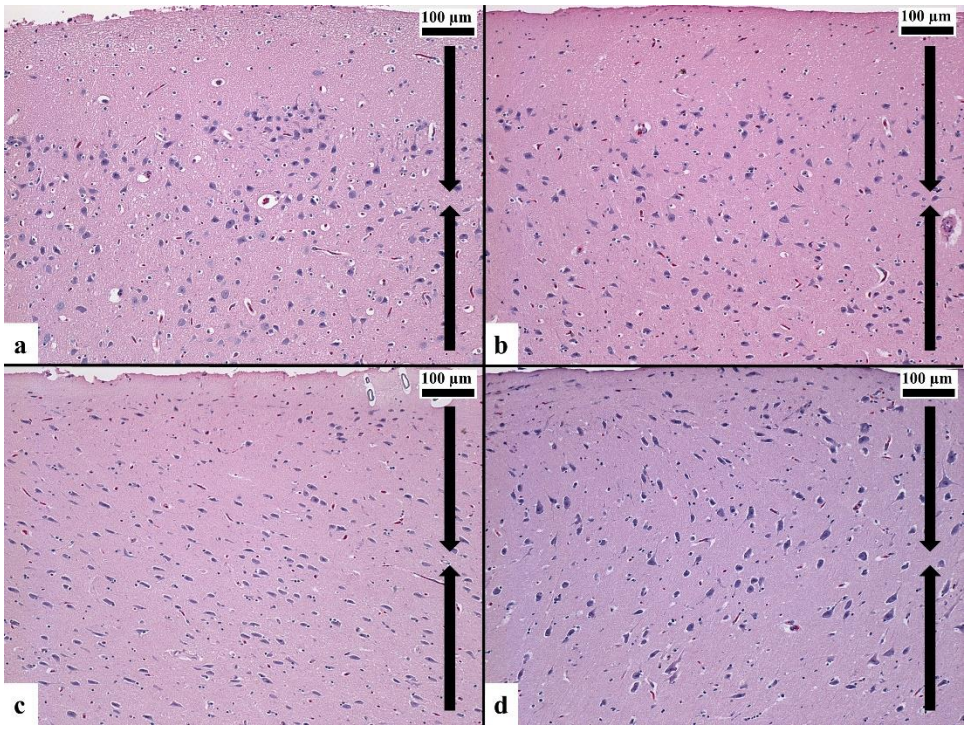

Figure 3.3 H&E stained brain tissue compressed at 800 s^{-1}: (a) An uncompressed control sample, (b) Interruption at 15% strain, (c) Interruption at 30% strain, and (d) Interruption at 40% strain.

The arrows on each image indicate the direction of compressive loading. A scale bar is included for reference. All images were taken at 10x magnification.

www.manaraa.com

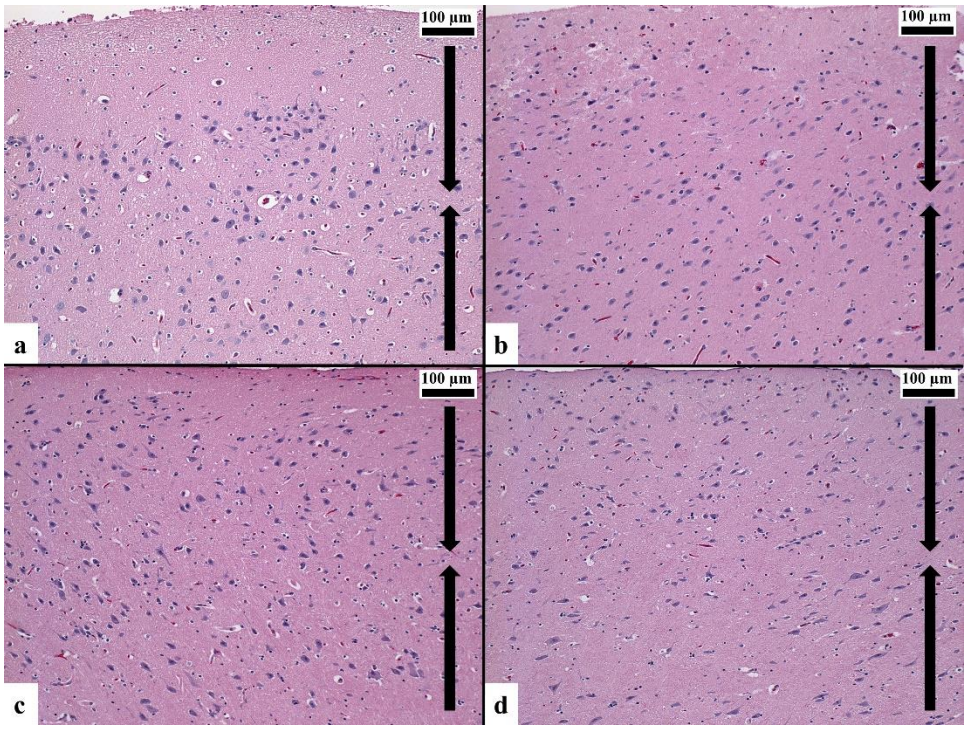

Figure 3.4 H&E stained brain tissue compressed at 900 s^{-1}: (a) An uncompressed control sample, (b) Interruption at 15% strain, (c) Interruption at 30% strain, and (d) Interruption at 40% strain.

The arrows on each image indicate the direction of compressive loading. A scale bar is included for reference. All images were taken at 10x magnification.

www.manaraa.com

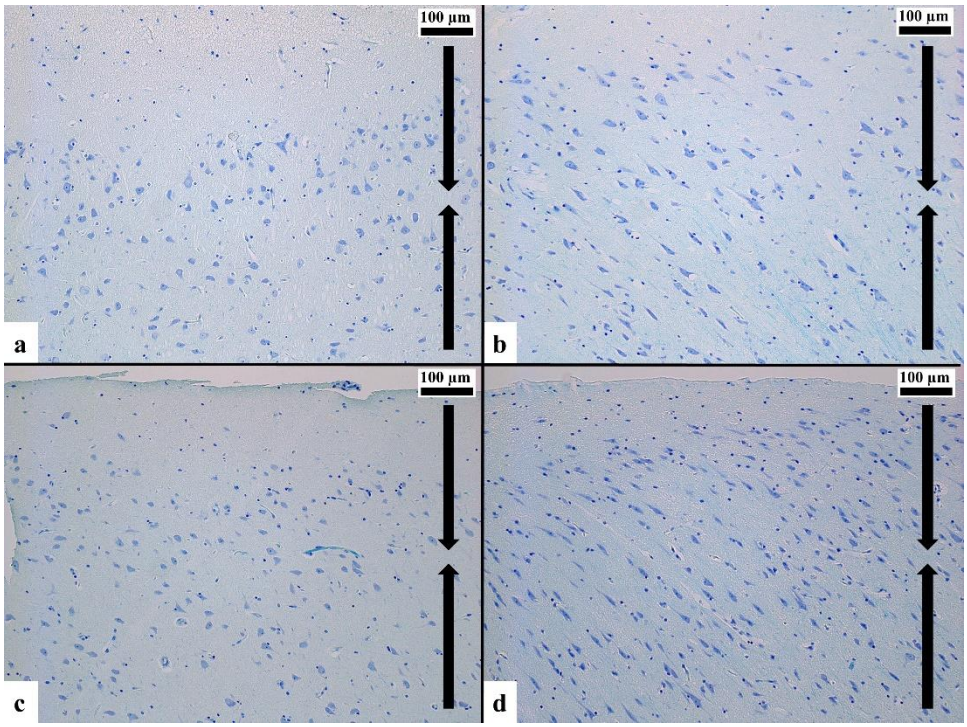

Figure 3.5 LFB stained brain tissue compressed at 650 s^{-1}: (a) An uncompressed control sample, (b) Interruption at 15% strain, (c) Interruption at 30% strain, and (d) Interruption at 40% strain.

The arrows on each image indicate the direction of compressive loading. A scale bar is included for reference. All images were taken at 10x magnification.

www.manaraa.com

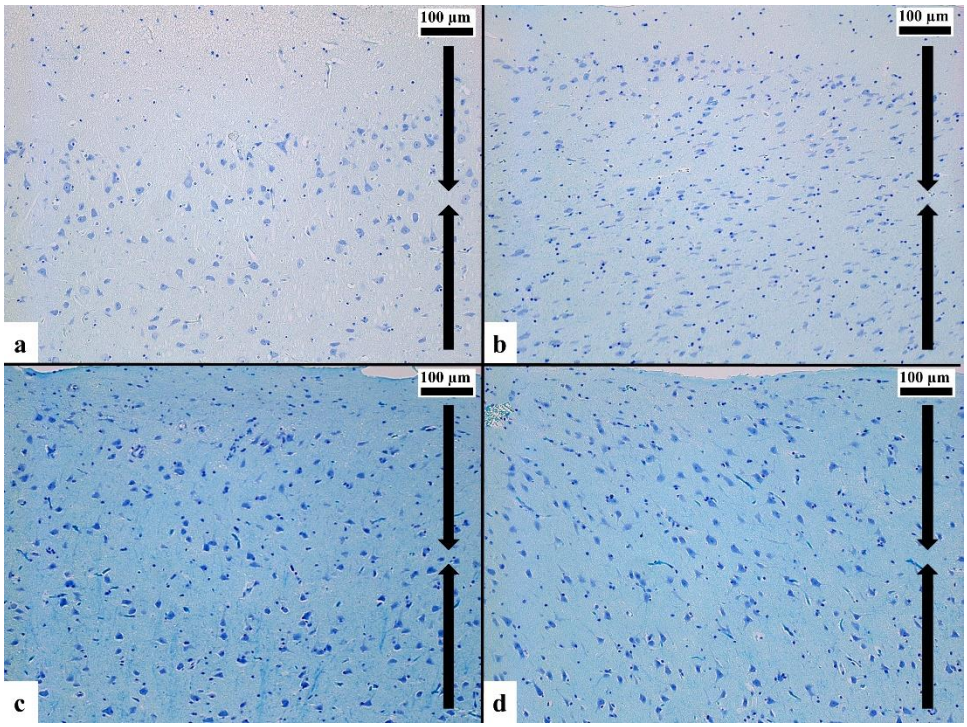

Figure 3.6 LFB stained brain tissue compressed at 800 s^{-1}: (a) An uncompressed control sample, (b) Interruption at 15% strain, (c) Interruption at 30% strain, and (d) Interruption at 40% strain.

The arrows on each image indicate the direction of compressive loading. A scale bar is included for reference. All images were taken at 10x magnification.

www.manaraa.com

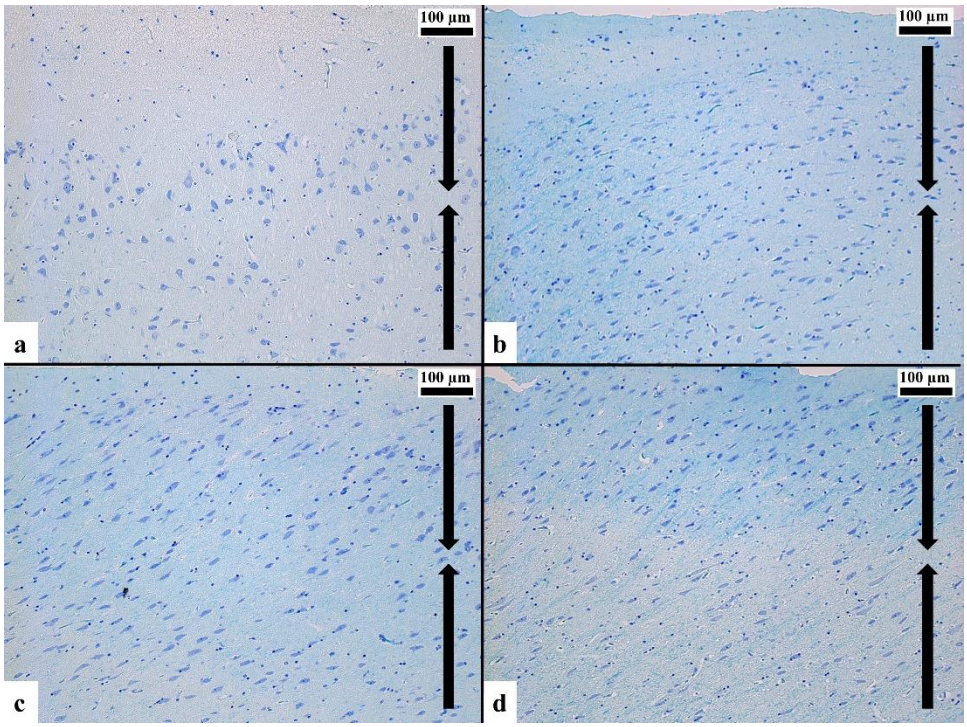

Figure 3.7 LFB stained brain tissue compressed at 900 s^{-1}: (a) An uncompressed control sample, (b) Interruption at 15% strain, (c) Interruption at 30% strain, and (d) Interruption at 40% strain.

The arrows on each image indicate the direction of compressive loading. A scale bar is included for reference. All images were taken at 10x magnification.

www.manaraa.com

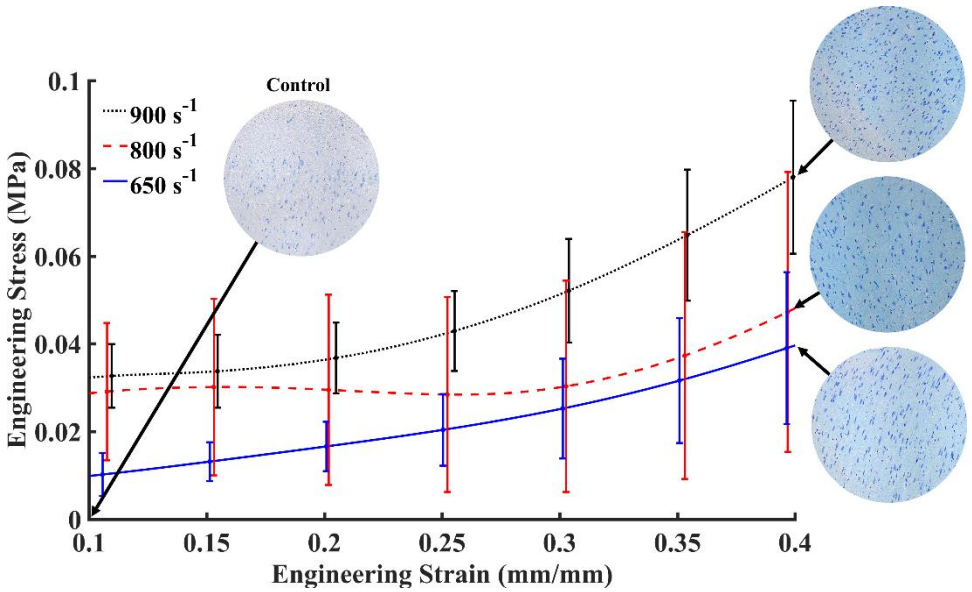

Figure 3.8 Engineering stress-strain response of brain tissue with corresponding micrographs.

Micrographs are of the control sample and samples compressed to 40% strain at rates of 650 s^{-1}, 800 s^{-1}, and 900 s^{-1}. Experimental standard deviation is expressed by error bars.

www.manaraa.com

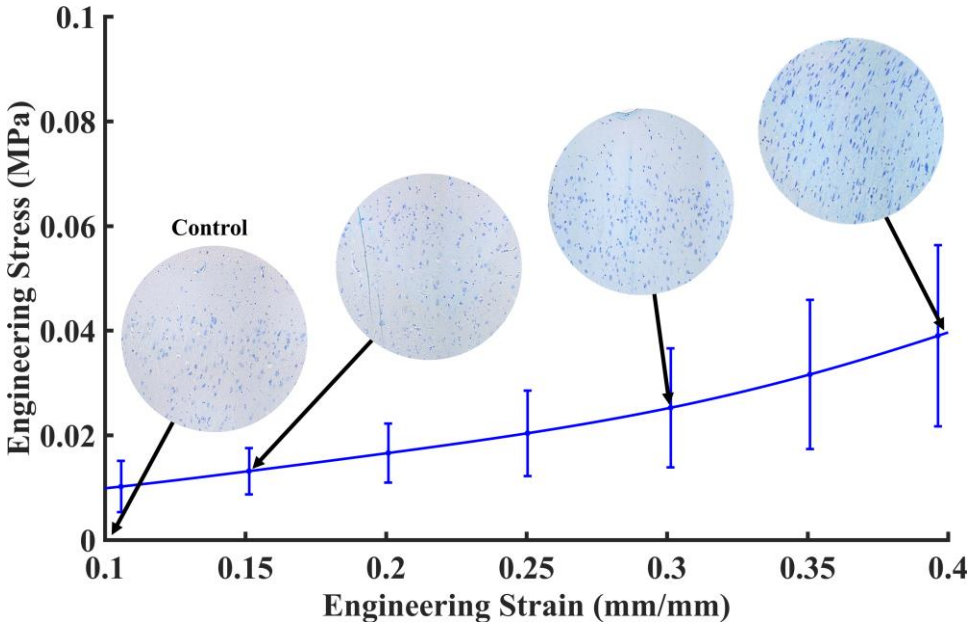

Figure 3.9 Engineering stress-strain response of porcine brain tissue compressed at 650 s^{-1} with corresponding micrographs.

Micrographs are of the control sample and samples compressed to strain levels of 15%, 30%, and 40%. Experimental standard deviation is expressed by error bars.

www.manaraa.com

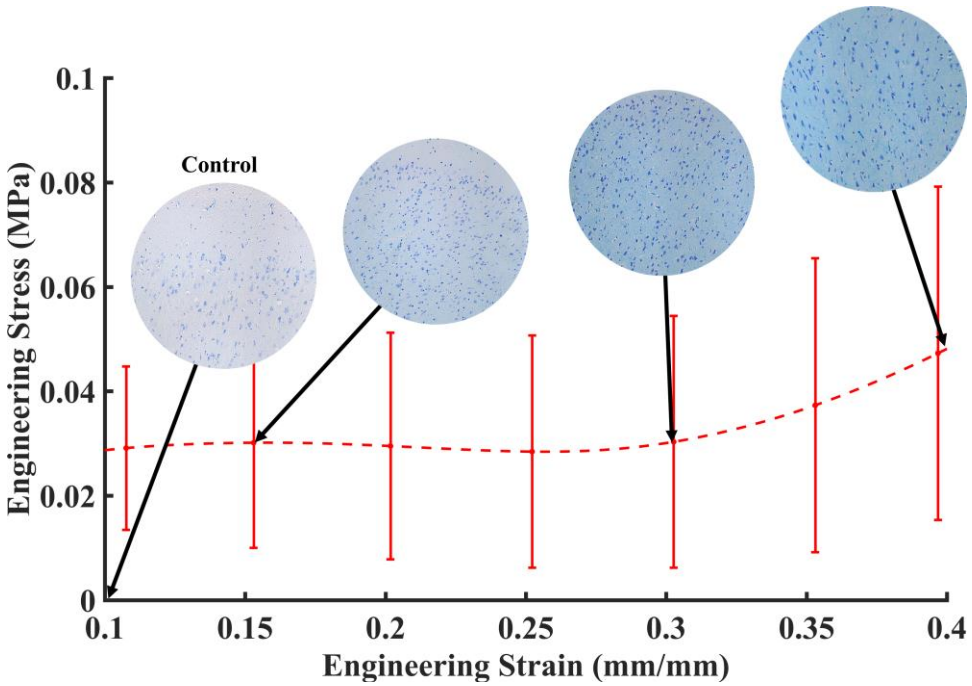

Figure 3.10 Engineering stress-strain response of porcine brain tissue compressed at 800 s^{-1} with corresponding micrographs.

Micrographs are of the control sample and samples compressed to strain levels of 15%, 30%, and 40%. Experimental standard deviation is expressed by error bars.

www.manaraa.com

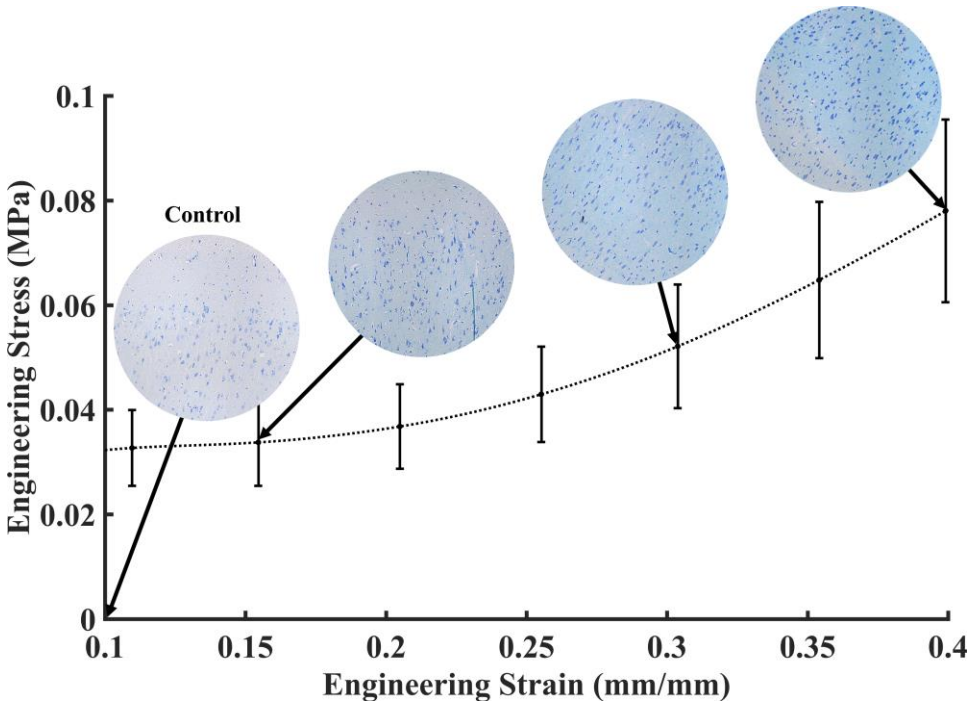

Figure 3.11 Engineering stress-strain response of porcine brain tissue compressed at 900 s^{-1} with corresponding micrographs.

Micrographs are of the control sample and samples compressed to strain levels of 15%, 30%, and 40%. Experimental standard deviation is expressed by error bars.

3.3 Image Analysis

The area fractions of the neuronal and glial cells from the various images were grouped together based on strain rate and strain level then averaged. The results are given in Table 3.3. The area fraction of the undamaged/control tissue was the lowest with a value of 3.05 ± 0.87%. As the tissue was compressed to higher levels of strain, the area fraction values increased. 4.60 ± 0.53%, 5.12 ± 0.29%, and 6.28 ± 0.72% were the area fractions of samples compressed at a rate of 650 s^{-1} to levels of 15, 30, and 40%, respectively. Additionally, increasing the strain rate at which the samples were compressed caused the area fractions to increase even further. Samples compressed at the

www.manaraa.com

strain rate of 900 s^{-1} to levels of 15, 30, and 40% expressed cellular area fractions of 6.65 ± 1.20%, 7.03 ± 0.44%, and 7.23 ± 1.11%. The values for the various area fractions are graphically represented using the bar chart in Figure 3.12.

Table 3.3 Area fractions of neuron and glial cells.

Strain Rate	Undamaged Control	15% Strain	30% Strain	40% Strain
-	3.05 ± 0.87	-	-	-
650 (s^{-1})	-	4.60 ± 0.53	5.12 ± 0.29	6.28 ± 0.72
800 (s^{-1})	-	6.47 ± 0.77	6.62 ± 0.41	7.04 ± 0.24
900 (s^{-1})	-	6.65 ± 1.20	7.03 ± 0.44	7.23 ± 1.11

Area fraction values were determined by averaging the area fractions of neuron and glial cells from micrographs (n = 3). Values are paired based on strain rate and strain level.

www.manaraa.com

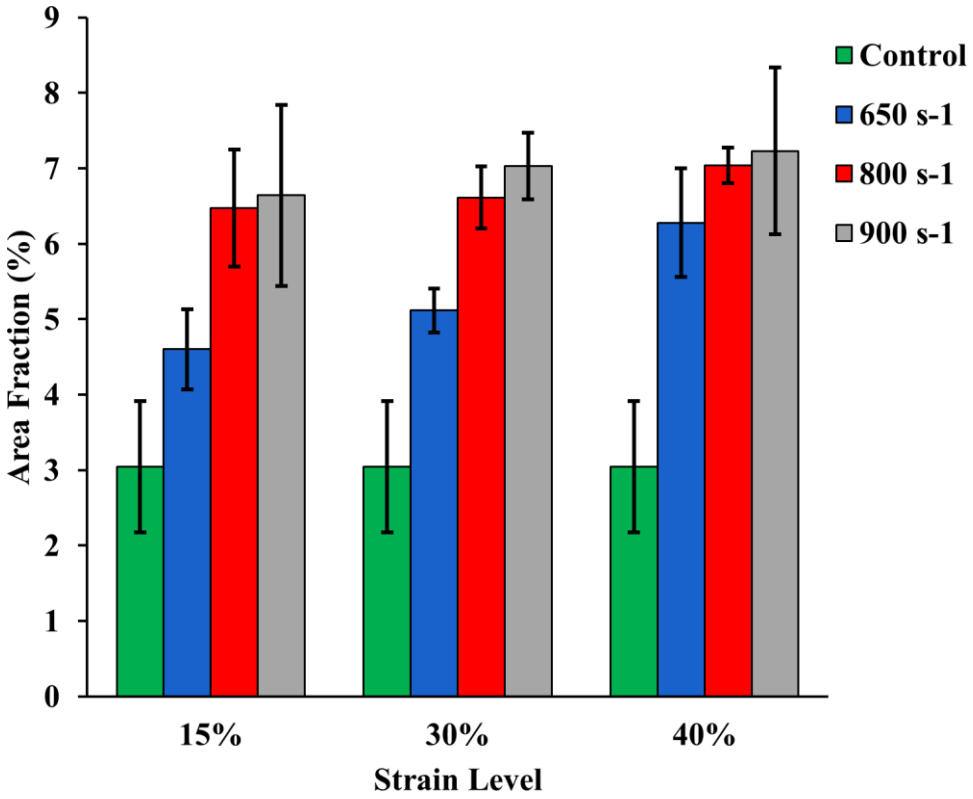

Figure 3.12 Bar chart of area fraction values.

The control value is included in each strain level grouping for comparison. The error bars represent standard deviation.

Statistical analysis was performed on the area fractions to determine their statistical significance. A Student's t-test was performed in order to compare the area fractions of the undamaged samples to the area fractions of the samples compressed to each strain level at each of the strain rates. The analysis returned p values <0.05 for all the strain level and strain rate pairings when compared to the control. The α value for the analysis was 0.05. A one-way ANOVA was performed on strain rate pairings of area fraction values using an α value of 0.1. There was a significant difference between the area fractions of strain rate pairings of 650 s^{-1} versus 800 s^{-1} and 650 s^{-1} versus 900 s^{-1} at 15% strain as the p values <0.1. However, the strain rate pairing of 800 s^{-1} versus 900 s^{-1}

www.manaraa.com

did not exhibit a significant difference between area fraction values. Similar statistical results were seen at the pairings in the 30% strain level category. Once the samples were compressed to the 40% strain level, there was no longer any statistical significance observed between the area fractions of the three strain rate pairings. However, the trend among the pairings continued with 650 s^{-1} versus 800 s^{-1} and 650 s^{-1} versus 700 s^{-1} having lower *p* values than the strain rate pairing of 800 s^{-1} and 900 s^{-1}. All the results of the statistical analysis are summarized in Table 3.4. A two-way ANOVA was also performed using area fraction as the dependent variable, and strain rate and strain level were the independent variables. The α value was 0.05. The *p* values for strain rate and strain level were <0.001 and 0.036, respectively. This indicates that the strain rate the samples were compressed at had slightly more effect on the microstructural compaction of the tissue.

www.manaraa.com

Table 3.4 Summary of *p* values obtained for area fractions corresponding to different strain rate pairings.

Area Fraction	Pairings	*p* Value
15%	[1] vs. [2]	0.026*
	[2] vs. [3]	0.845
	[1] vs. [3]	0.054*
30%	[1] vs. [2]	0.007*
	[2] vs. [3]	0.298
	[1] vs. [3]	0.003*
40%	[1] vs. [2]	0.159
	[2] vs. [3]	0.780
	[1] vs. [3]	0.280

Strain rates are labeled so that [1] = 650 s^{-1}, [2] = 800 s^{-1}, and [3] = 900 s^{-1} with $\alpha = 0.10$. (*) indicates significant values.

www.manaraa.com

CHAPTER IV

DISCUSSION

The primary focus of this research was to develop a novel testing methodology for interrupting high rate compression performed on brain tissue at specific deformation states or levels of strain. Success of such a testing method prevented total tissue destruction during testing and would allow for samples to be prepared for histological staining and analysis. Interruption tests on biological tissues were possible in the cases of the studies by Begonia, et al. and Weed, et al. due to the fact that they both performed quasi-static testing using the Mach-1 Micromechanical Testing System (Biomomentum, Quebec, CA) (Begonia et al., 2010; Weed et al., 2012). The platen displacement on this type of stepper-motor driven testing device is precisely controlled and thus the strain level of each sample is controlled under the same precision. On the contrary, the SHPB's motion is initiated by the pressure released from a compressed air tank and its control is based on laws of physics. Meaning, once a test is initiated on the SHPB, it will continue until external forces are high enough to cause the bars to stop. In the case of soft biological tissues, this usually results in total destruction of samples. This lack of fine control requires special modifications to the SHPB in order to perform interruption tests. Interruption tests using a SHPB have been performed on metal samples undergoing tensile loading with the use of specially-crafted interruption devices (Dongfang et al., 2010; Yang et al., 2014). Once custom-sized samples had elongated to a predetermined

www.manaraa.com

amount of strain, they would make contact with the interruption devices and fracture at specific locations. This type of approach was part of the inspiration that led to the final design of the interruption attachments developed for this study. The combination of specific and consistent sample sizes with interruption attachments that would interact with one another during testing allowed for successful interruption tests that preserved the samples for further analysis.

When studying brain tissue mechanics to apply the gathered information towards efforts to better understand and prevent TBI in human patients, it is most ideal and beneficial to use human tissues during testing. However, the logistics and protocols involved in acquiring samples from human patients would greatly hinder research progress due to lack of accessibility. With a study, such as this one, that involves repeatable testing procedures, it is much more practical to use an animal model for *in vitro* testing. Porcine tissue has been widely used in other biomechanical studies because of its similarities to various human tissues, especially, brain (Song et al., 2007; Begonia et al., 2010; Prabhu et al., 2011; Thibault P Prevost et al., 2011; Thibault P. Prevost et al., 2011; Trexler et al., 2011; Zhang et al., 2011; Clemmer et al., 2016). The porcine brain has similar mechanical properties to that of a human brain and is more readily available than other laboratory animals (Galford and McElhaney, 1970; Miller et al., 2000; Miller and Chinzei, 2002). The development of the human and porcine CNS is also comparable (Dickerson and Dobbing, 1967; Lind et al., 2007). Additionally, the close proximity of an abattoir to the testing facilities allowed for a constant supply of fresh samples to maintain consistent post mortem test times thus helping to reduce any variations in the results due

www.manaraa.com

to tissue degradation. All of these factors lead to porcine tissue being an effective surrogate for human brain in this study.

Results from the stress-strain analysis of the porcine brain indicate that the tissue exhibits a strain rate dependent viscoelastic mechanical response, which is consistent with findings in previous studies (Miller, 2000; Miller et al., 2000; Miller and Chinzei, 2002; Velardi et al., 2006; Tamura et al., 2008; Pervin and Chen, 2009; Begonia et al., 2010; Thibault P. Prevost et al., 2011; Prabhu et al., 2011; Thibault P Prevost et al., 2011; Rashid et al., 2012; Clemmer et al., 2016). This mechanical response is easily explained by examining the makeup of neural tissue. Brain has long been presumed to be an incompressible material due to its large water content of up to 80% in specific regions (Neeb et al., 2008; Libertiaux et al., 2011). The elastic region of the stress-strain curve is due to the response of the cellular components and axons in the brain tissue. At higher levels of strain, it is likely that the axons become more tightly packed and cause a stiffening effect in the mechanical response.

The values from Table 3.3 show a progressive increase in area fraction percentage of the neural constituents as the brain tissue samples are compressed to higher levels of strain when compared to the area fraction of the control. All these values were determined to be statistically different when compared to the control area fraction, indicating that tissue deformation was indeed occurring in the interrupted samples. This deformation is likely due to the cross-sectional area of the samples being reduced as they are being compressed. As the strain level increases, the cross-sectional area decreases. This forces the cells and the extracellular matrix in the brain tissue to become compacted and reshaped as they are forced to occupy a smaller area. This forces the cells closer

www.manaraa.com

together unlike the loosely spaced structure seen in the control samples. Measuring the area fraction allowed for capturing of this phenomenon, because the cells in the compressed tissue make up a larger percentage of the cross-sectional area as witnessed in the micrographs. The results of the two-way ANOVA, where area fraction was set as the dependent variable and strain level and strain rate were the two independent variables, provide further evidence to this microstructural response. The *p* value for strain level was 0.036 with α=0.05, indicating a significant change in area fraction as the samples were compressed to higher strain levels. There is also a noticeable increase of area fractions between groups of tissue compressed at different strain rates to the same strain level. As the rate of compression increases, it forces the tissue to conform to its new dimensions faster. The values from Table 3.4 indicate a significant increase between the area fractions of samples compressed to 15% and 30% strain when comparing 650 s^{-1} to 800 s^{-1} and 650 s^{-1} to 900 s^{-1}. However, there was no significant difference between area fractions of samples compressed at rates of 800 s^{-1} and 900 s^{-1} at those strain levels. This is most likely due to those two strain rates being similar when considering the range of high rates associated with SHPB testing. Although these trends continued with the area fractions of samples compressed to levels of 40% strain, there was no significant difference between the different strain rate pairings. Even with these findings about strain rate influence among the various pairings, results from the two-way ANOVA indicate that strain rate was a significant influence over the amount of tissue deformation.

The trends in the image analysis results are comparable to those found by Begonia et al.; however, there are differences in the quantitative aspects of the neuronal constituent evolution due to deformation (Begonia et al., 2010). Begonia et al. observed a

www.manaraa.com

control area fraction of 7.85 ± 0.07%, but the area fractions increased to 11.55 ± 0.35%, 13.30 ± 0.28%, and 19.50 ± 0.14% when compressed to 40% strain at rates of 0.00625 s^{-1}, 0.025 s^{-1}, and 0.10 s^{-1}, respectively (Begonia et al., 2010). These values share the same trend with the area fractions in the present study and indicate increased compaction of the neural constituents when the tissue is subjected to strains at increasing rates. However, the actual values of the area fractions observed by Begonia et al. are significantly larger in magnitude (Begonia et al., 2010). These differences can likely be attributed to the differences in staining protocols and microscopy techniques used. These differences would lead to varying representations of the observed neural structures. Additionally, different variations between the area fractions of the interrupted samples can be explained by the use of strain rates from the quasi-static range in the previous study (Begonia et al., 2010).

Considering that the exact same piece of tissue is not being tested within each category could present some data misrepresentation. Several studies have noted that specimen-to-specimen variations in the sample mechanical properties and morphology are significant for biological tissues (Estes and McElhaney, 1970; Miller and Chinzei, 1997). This aspect of variation is further exemplified in accidents to humans, who go through very similar injury scenarios or external boundary conditions, but end with up different TBI-related pathologies (Andriessen et al., 2010; Majdan et al., 2013). To help minimize differences in the results, samples were extracted in similar parts of the brain from the parietal and frontal regions. However, some variation and differences in neuronal makeup are expected between each sample due to the use of multiple test subjects.

www.manaraa.com

The result of the mechanical testing (properties) and the microstructural analysis (structure) of the compressed brain tissue provides insight on how the structure of the tissue could possibly change as a result of mechanical insult. These relationships will be useful in better understanding the microstructural changes that occur in the brain under conditions that can lead to TBI. Previous studies have found that TBI is most likely to occur when brain is deformed beyond 20% strain and at rates greater than 10 s^{-1} (Bain and Meaney, 2000; Geddes and Cargill, 2001; Pfister et al., 2003). This provides justification for the range of strain levels and rates used in this study to analyze the brain's response to conditions that lead to severe TBI. One type of TBI that is often associated with high-rate loadings and deformation of the brain tissue is traumatic axonal injury (TAI). TAI is a result of inertial forces causing large amounts of stress on axons leading them to become severed or partially damaged. This leads to breakdown in communication between neurons due to a lack of a messaging pathway and causes the brain processes to malfunction (Johnson et al., 2013; Hill et al., 2016). Although TAI is typically associated with damage from shear stresses, these stresses are the result of high-velocity translational or rotational deformations in the brain. This results in the rearrangement of the neural tissue and its various components. Thus, the deformation seen when analyzing the microstructure of the tissues in this study can be used to approximate microstructural deformation under TBI conditions.

www.manaraa.com

CHAPTER V

CONCLUSIONS

The interruption technique developed in this study is an effective means to preserve tissue integrity during interrupted compression testing with the SHPB in order to analyze the microstructural damage that occurs. This technique can be applied to similar soft biological tissues such as lung, liver, muscle, etc. to gather information on their microstructural response to high strain rate deformation. While this method was sufficient enough for the purposes of this study, future improvements can be made. Since this was the first attempt at developing and testing these interruption attachments, the prototypes used in this study were fabricated by hand using a lathe. To ensure consistent product design, computer aided design (CAD) models could be developed and used to 3-D print or fabricate with the use of computer numerical control (CNC) perfectly consistent parts. These approaches would help to alleviate any human manufacturing errors and increase the speed of production of custom attachments when dealing with tissues that require special sample sizes for testing. Additionally, modifications can be made to the attachments that would allow for strain gages to capture the mechanical response of the tissue being interrupted. Currently, the design and function of the interruption attachments causes large noise outputs in the strain gage measurements as described in the Appendix. This prevents mechanics data capture during testing. Ideally, the tissue's response could be captured during the interruption tests. This would condense the overall

www.manaraa.com

methods involved with a study of this nature by removing the need for a two-part testing procedure.

The overarching goal of developing the interruption technique used in this study to analyze the microstructural damage that occurs to brain tissue under high strain rate deformation is to develop a structure-property relationship in the tissue. This information will lead to improvements in FE models that are used to increase safety in vehicles and equipment to prevent or mitigate the symptoms associated with TBI. This was first realized by Begonia et al., 2010, by interrupting brain tissue at quasi-static strain rates (Begonia et al., 2010). Although the information gathered in that study proved to be useful, the strain rates used were much lower than those that have been found to be associated with TBI, especially when considering TBI caused by blasts or severe automotive accidents. This study developed a technique to analyze tissues that have undergone high rate deformation on the SHPB. The structure-property relationships gathered from this study will help to advance the study of TBI by providing information gathered under real-world conditions.

www.manaraa.com

CHAPTER VI

FUTURE WORKS

To improve upon this study, further testing using the same methods on a wider range strain rates would be beneficial in evaluating brain's response at even higher strain rates. Previous studies, such as the one performed by Pervin and Chen, have tested the mechanical response of brain under loading rates up to 3,000 s^{-1} (Pervin and Chen, 2009). The strain rates between 650 s^{-1} and 900 s^{-1} are much more conservative, in comparison. These lower rates were used to more accurately control the loadings during compressive loading. Additionally, higher strain rates would have caused more force to be exerted on the interruption attachments and lead to potential destruction of the devices. Increased loading rates paired with the interruption testing methods would lead to more information into the microstructural response of the brain, but modifications, such as larger dimensions or different materials, may need to be made to the attachments in order to withstand the higher loadings.

Although brain was the focus of this study, various other tissues are subject to damage when exposed to high impact loadings. The lungs, liver, and heart are all vital organs that are susceptible to injury when exposed to conditions like those in a blast situation. Saraf et al. has already explored the mechanical response of these particular tissues under compressive and shear loadings using the SHPB (Saraf et al., 2007). The techniques used in the current study could be applied to these other tissues. Different

www.manaraa.com

analyses other than the measure of area fraction would likely need to be used on various other tissues due to their vastly different microstructure, but high-rate interruption testing would be useful in helping to develop structure-property relationships for them, as well. Successful testing with additional tissues would also help to further validate the interruption techniques used in this study.

www.manaraa.com

REFERENCES

Andriessen, T.M.J.C., Jacobs, B., Vos, P.E., 2010. Clinical characteristics and pathophysiological mechanisms of focal and diffuse traumatic brain injury. J. Cell. Mol. Med. 14, 2381–2392. doi:10.1111/j.1582-4934.2010.01164.x

Bain, A.C., Meaney, D.F., 2000. Tissue-Level Thresholds for Axonal Damage in an Experimental Model of Central Nervous System White Matter Injury. J. Biomech. Eng. 122, 615. doi:10.1115/1.1324667

Begonia, M.T., Prabhu, R., Liao, J., Horstemeyer, M.F., Williams, L.N., 2010. The Influence of Strain Rate Dependency on the Structure–Property Relations of Porcine Brain. Ann. Biomed. Eng. 38, 3043–3057. doi:10.1007/s10439-010-0072-9

Blumenfeld, H., 2010. Neuroanatomy Overview and Basic Definitions, in: Neuroanatomy through Clinical Cases. Sinauer Associates, Sunderland, Mass., pp. 13–46.

Chen, X., Sase, K., Konno, A., Tsujita, T., 2014. Identification of mechanical properties of brain parenchyma for brain surgery haptic simulation, in: 2014 IEEE International Conference on Robotics and Biomimetics (ROBIO 2014). IEEE, pp. 1656–1661. doi:10.1109/ROBIO.2014.7090572

Clemmer, J., Prabhu, R., Chen, J., Colebeck, E., Priddy, L.B., McCollum, M., Brazile, B., Whittington, W., Wardlaw, J.L., Rhee, H., Horstemeyer, M.F., Williams, L.N., Liao, J., 2016. Experimental observation of high strain rate responses of porcine brain, liver, and tendon. J. Mech. Med. Biol. 16, 1650032. doi:10.1142/S0219519416500329

Dickerson, J.W.T., Dobbing, J., 1967. Prenatal and Postnatal Growth and Development of the Central Nervous System of the Pig. Proc. R. Soc. B Biol. Sci. 166, 384–395. doi:10.1098/rspb.1967.0002

Dongfang, M., Danian, C., Shanxing, W., Huanran, W., Yanjun, H., Canyuan, C., 2010. An interrupted tensile testing at high strain rates for pure copper bars. J. Appl. Phys. 108, 114902. doi:10.1063/1.3516475

Estes, M.S., McElhaney, J.H., 1970. Response of brain tissue of compressive loading. ASME Pap. No. 70-BHF-13.

www.manaraa.com

Faul, M., Xu, L., Wald, M.M., Coronado, V.G., 2010. Traumatic brain injury in the United States: emergency department visits, hospitalizations, and deaths, 2002-2006. U.S. Department of Health and Human Services, Centers for Disease Control and Prevention, National Center for Injury Prevention and Control, Atlanta, Ga.

Fischer, H., 2014. A Guide to U.S. Military Casualty Statistics: Operation New Dawn, Operation Iraqi Freedom, and Operation Enduring Freedom, Congressional Research Service.

Francis, D.K., Whittington, W.R., Lawrimore, W.B., Allison, P.G., Turnage, S.A., Bhattacharyya, J.J., 2017. Split Hopkinson Pressure Bar Graphical Analysis Tool. Exp. Mech. 57, 179–183. doi:10.1007/s11340-016-0191-9

Galford, J.E., McElhaney, J.H., 1970. A viscoelastic study of scalp, brain, and dura. J. Biomech. 3, 211–221. doi:10.1016/0021-9290(70)90007-2

Geddes, D.M., Cargill, R.S., 2001. An in Vitro Model of Neural Trauma: Device Characterization and Calcium Response to Mechanical Stretch. J. Biomech. Eng. 123, 247. doi:10.1115/1.1374201

Hill, C.S., Coleman, M.P., Menon, D.K., 2016. Traumatic Axonal Injury: Mechanisms and Translational Opportunities. Trends Neurosci. doi:10.1016/j.tins.2016.03.002

Hopkinson, B., 1914. A Method of Measuring the Pressure Produced in the Detonation of High Explosives or by the Impact of Bullets. Philos. Trans. R. Soc. A Math. Phys. Eng. Sci. 213, 437–456. doi:10.1098/rsta.1914.0010

Jeronimidis, G., 2000. Structure-Property Relationships in Biological Materials, in: Elices, M. (Ed.), Structural Biological Materials: Design and Structure-Property Relationships. Elsevier Science, Kidlington, Oxford, pp. 1–16.

Johnson, V.E., Stewart, W., Smith, D.H., 2013. Axonal pathology in traumatic brain injury. Exp. Neurol. 246, 35–43. doi:10.1016/j.expneurol.2012.01.013

Kay, T., Harrington, D.E., Adams, R., Anderson, T., Berrol, S., Cicerone, K., Dahlberg, C., Gerber, D., Goka, R., Harley, P., Hilt, J., Horn, L., Lehmkuhl, D., Malec, J., 1993. Definition of mild traumatic brain injury. J. Head Trauma Rehabil. 8, 86–87. doi:10.1097/00001199-199309000-00010

Kolsky, H., 1949. An Investigation of the Mechanical Properties of Materials at very High Rates of Loading. Proc. Phys. Soc. Sect. B 62, 676–700. doi:10.1088/0370-1301/62/11/302

Libertiaux, V., Pascon, F., Cescotto, S., 2011. Experimental verification of brain tissue incompressibility using digital image correlation. J. Mech. Behav. Biomed. Mater. 4, 1177–1185. doi:10.1016/j.jmbbm.2011.03.028

www.manaraa.com

Lind, N.M., Moustgaard, A., Jelsing, J., Vajta, G., Cumming, P., Hansen, A.K., 2007. The use of pigs in neuroscience: Modeling brain disorders. Neurosci. Biobehav. Rev. 31, 728–751. doi:10.1016/j.neubiorev.2007.02.003

Majdan, M., Mauritz, W., Wilbacher, I., Janciak, I., Brazinova, A., Rusnak, M., Leitgeb, J., 2013. Traumatic brain injuries caused by traffic accidents in five European countries: outcome and public health consequences. Eur. J. Public Health 23, 682–687. doi:10.1093/eurpub/cks074

Miller, K., 2000. Biomechanics of soft tissues. Med. Sci. Monit. 6, 158–67.

Miller, K., 1999. Constitutive model of brain tissue suitable for finite element analysis of surgical procedures. J. Biomech. 32, 531–537. doi:10.1016/S0021-9290(99)00010-X

Miller, K., Chinzei, K., 2002. Mechanical properties of brain tissue in tension. J. Biomech. 35, 483–490. doi:10.1016/S0021-9290(01)00234-2

Miller, K., Chinzei, K., 1997. Constitutive modelling of brain tissue: Experiment and theory. J. Biomech. 30, 1115–1121. doi:10.1016/S0021-9290(97)00092-4

Miller, K., Chinzei, K., Orssengo, G., Bednarz, P., 2000. Mechanical properties of brain tissue in-vivo: experiment and computer simulation. J. Biomech. 33, 1369–1376. doi:10.1016/S0021-9290(00)00120-2

Neeb, H., Ermer, V., Stocker, T., Shah, N.J., 2008. Fast quantitative mapping of absolute water content with full brain coverage. Neuroimage 42, 1094–1109. doi:10.1016/j.neuroimage.2008.03.060

Okie, S., 2005. Traumatic Brain Injury in the War Zone. N. Engl. J. Med. 352, 2043–2047. doi:10.1056/NEJMp058102

Pervin, F., Chen, W.W., 2009. Dynamic mechanical response of bovine gray matter and white matter brain tissues under compression. J. Biomech. 42, 731–735. doi:10.1016/j.jbiomech.2009.01.023

Pfister, B.J., Weihs, T.P., Betenbaugh, M., Bao, G., 2003. An In Vitro Uniaxial Stretch Model for Axonal Injury. Ann. Biomed. Eng. 31, 589–598. doi:10.1114/1.1566445

Prabhu, R., Horstemeyer, M.F., Tucker, M.T., Marin, E.B., Bouvard, J.L., Sherburn, J.A., Liao, J., Williams, L.N., 2011. Coupled experiment/finite element analysis on the mechanical response of porcine brain under high strain rates. J. Mech. Behav. Biomed. Mater. 4, 1067–1080. doi:10.1016/j.jmbbm.2011.03.015

Prevost, T.P., Balakrishnan, A., Suresh, S., Socrate, S., 2011. Biomechanics of brain tissue. Acta Biomater. 7, 83–95. doi:10.1016/j.actbio.2010.06.035

www.manaraa.com

Prevost, T.P., Jin, G., de Moya, M.A., Alam, H.B., Suresh, S., Socrate, S., 2011. Dynamic mechanical response of brain tissue in indentation in vivo, in situ and in vitro. Acta Biomater. 7, 4090–4101. doi:10.1016/j.actbio.2011.06.032

Rashid, B., Destrade, M., Gilchrist, M.D., 2012. Mechanical characterization of brain tissue in compression at dynamic strain rates. J. Mech. Behav. Biomed. Mater. 10, 23–38. doi:10.1016/j.jmbbm.2012.01.022

Risdall, J.E., Menon, D.K., 2011. Traumatic brain injury. Philos. Trans. R. Soc. B Biol. Sci. 366, 241–250. doi:10.1098/rstb.2010.0230

Rosenfeld, J. V., McFarlane, A.C., Bragge, P., Armonda, R.A., Grimes, J.B., Ling, G.S., 2013. Blast-related traumatic brain injury. Lancet Neurol. 12, 882–893. doi:10.1016/S1474-4422(13)70161-3

Saraf, H., Ramesh, K.T., Lennon, A.M., Merkle, A.C., Roberts, J.C., 2007. Mechanical properties of soft human tissues under dynamic loading. J. Biomech. 40, 1960–1967. doi:10.1016/j.jbiomech.2006.09.021

Sharma, A., Shukla, A., Prosser, R.A., 2002. Mechanical characterization of soft materials using high speed photography and split hopkinson pressure bar technique. J. Mater. Sci. 37, 1005–1017. doi:10.1023/A:1014308216966

Song, B., Chen, W., Ge, Y., Weerasooriya, T., 2007. Dynamic and quasi-static compressive response of porcine muscle. J. Biomech. 40, 2999–3005. doi:10.1016/j.jbiomech.2007.02.001

Tamura, A., Hayashi, S., Watanabe, I., Nagayama, K., Matsumoto, T., 2008. Mechanical Characterization of Brain Tissue in High-Rate Extension. J. Biomech. Sci. Eng. 3, 263–274. doi:10.1299/jbse.3.263

Thibodeau, G., Patton, K., 2008. The Nervous System, in: Structure & Function of the Body. Mosby Elsevier, St. Louis, Missouri, pp. 184–225.

Trexler, M.M., Lennon, A.M., Wickwire, A.C., Harrigan, T.P., Luong, Q.T., Graham, J.L., Maisano, A.J., Roberts, J.C., Merkle, A.C., 2011. Verification and implementation of a modified split Hopkinson pressure bar technique for characterizing biological tissue and soft biosimulant materials under dynamic shear loading. J. Mech. Behav. Biomed. Mater. 4, 1920–1928. doi:10.1016/j.jmbbm.2011.06.008

van Dommelen, J.A.W., van der Sande, T.P.J., Hrapko, M., Peters, G.W.M., 2010. Mechanical properties of brain tissue by indentation: Interregional variation. J. Mech. Behav. Biomed. Mater. 3, 158–166. doi:10.1016/j.jmbbm.2009.09.001

www.manaraa.com

Van Sligtenhorst, C., Cronin, D.S., Wayne Brodland, G., 2006. High strain rate compressive properties of bovine muscle tissue determined using a split Hopkinson bar apparatus. J. Biomech. 39, 1852–1858. doi:10.1016/j.jbiomech.2005.05.015

Velardi, F., Fraternali, F., Angelillo, M., 2006. Anisotropic constitutive equations and experimental tensile behavior of brain tissue. Biomech. Model. Mechanobiol. 5, 53–61. doi:10.1007/s10237-005-0007-9

Weed, B.C., Borazjani, A., Patnaik, S.S., Prabhu, R., Horstemeyer, M.F., Ryan, P.L., Franz, T., Williams, L.N., Liao, J., 2012. Stress State and Strain Rate Dependence of the Human Placenta. Ann. Biomed. Eng. 40, 2255–2265. doi:10.1007/s10439-012-0588-2

Williams, S.M., White, L.E., 2013. Sylvius 4 Online. Sinauer Associates, Sunderland, Mass.

Yang, X., Xiong, X., Yin, Z., Wang, H., Wang, J., Chen, D., 2014. Interrupted Test of Advanced High Strength Steel with Tensile Split Hopkinson Bar Method. Exp. Mech. 54, 641–652. doi:10.1007/s11340-013-9828-0

Zhang, J., Yoganandan, N., Pintar, F.A., Guan, Y., Shender, B., Paskoff, G., Laud, P., 2011. Effects of tissue preservation temperature on high strain-rate material properties of brain. J. Biomech. 44, 391–396. doi:10.1016/j.jbiomech.2010.10.024

Zhao, H., Gary, G., Klepaczko, J.R., 1997. On the use of a viscoelastic split hopkinson pressure bar. Int. J. Impact Eng. 19, 319–330. doi:10.1016/S0734-743X(96)00038-3

www.manaraa.com

APPENDIX A

SHPB TESTING

www.manaraa.com

An example of the strain gage response from a test to determine the brain tissue's mechanical response is give in Figure A.1. It was this data that was used with the Split Hopkinson Pressure Bar Graphical Analysis Tool shown in Figure A.2 to produce the stress-strain data in Figures 3.8-3.11 (Francis et al., 2017). A sample strain gage response from a SHPB test with the interruption attachments in place can be seen in Figure A.3. Due to the noise caused from the impact of the attachments as they came in contact with one another and allowed for interruption of the compression tests, data could not be acquired to determine the mechanical response of the brain tissue during this testing procedure. This was the justification for performing full compression tests to failure separately to acquire stress-strain data for the brain tissue. The combination of the mechanical data from the full compression tests and the histological images from the interruption tests allowed for a structure-property relationship to be developed.

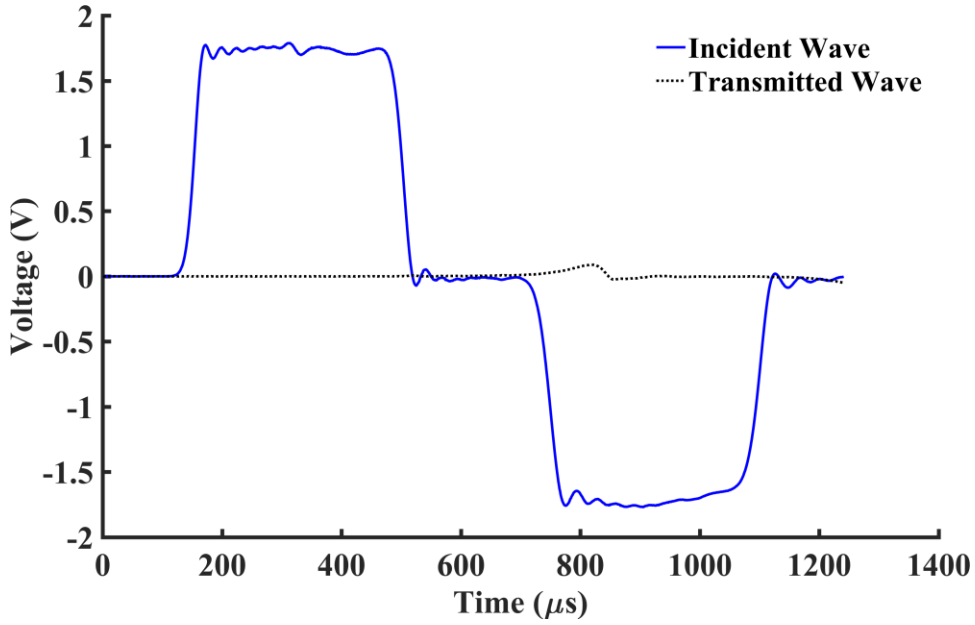

Figure A.1 Typical strain gage response from a full compression test to failure on the SHPB.

www.manaraa.com

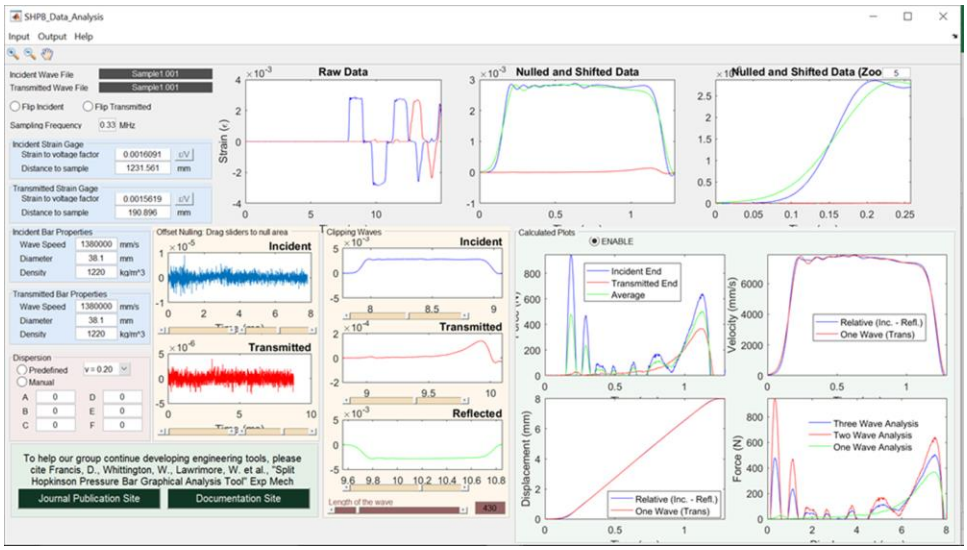

Figure A.2 SHPB Graphical Analysis Tool window.

The SHPB Graphical Analysis Tool allowed for efficient analysis of the strain gage data acquired during testing using the multiple output windows shown in the figure (Francis et al., 2017).

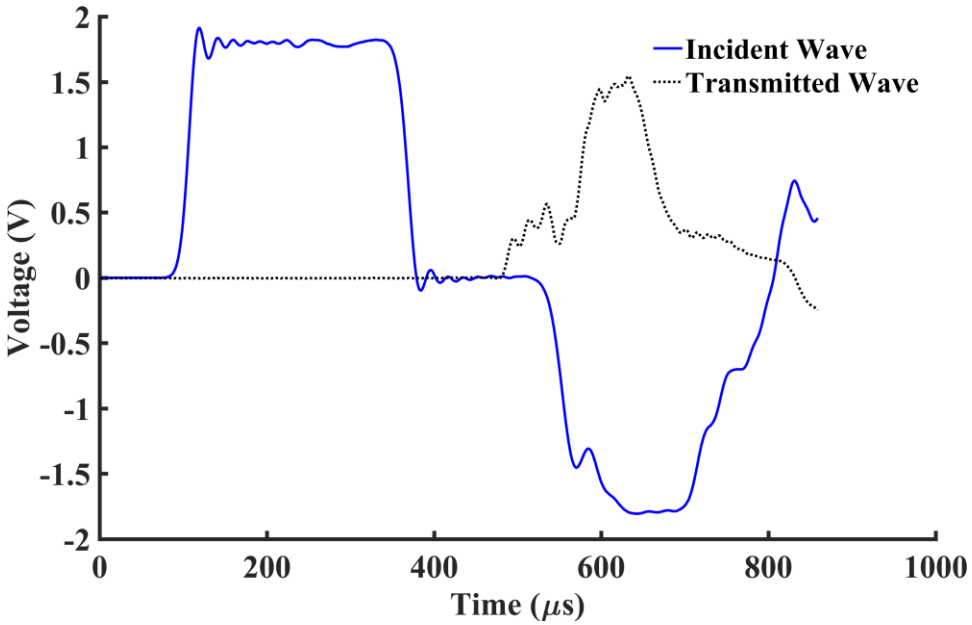

Figure A.3 Typical strain gage response from an interruption test on the SHPB.

Noise caused by the interruption attachments is evident in the transmitted and reflected waves. This masked the brain tissue response.

www.manaraa.com

APPENDIX B

IMAGE ANALYSIS

www.manaraa.com

The sizes the micrographs of the interrupted samples needed to be cropped to were determined by using

$$\nu = -\frac{\varepsilon_y}{\varepsilon_x} \tag{B.1}$$

to determine the amount of lateral strain that the samples' cross-section underwent during compression where ν is Poisson's ratio, ε_y is longitudinal strain, and ε_x is lateral strain. This percentage deformation for each of the different strain level cases was proportionately applied to the micrographs based on the control images' pixel size to determine appropriate dimensions for the interrupted micrographs.

www.manaraa.com